Tampere University

Khanh Ma

IMPLEMENTATION AND EVALUATION OF COMMUNICATION SYSTEM FOR AUTONOMOUS OFFSHORE VEHICLES

Faculty of Information Technology and Communication Sciences (ITC)
Master's thesis
November 2020

Abstract

Khanh Ma: IMPLEMENTATION AND EVALUATION OF COMMUNICATION SYSTEM FOR AUTONOMOUS OFFSHORE VEHICLES
Master's thesis
Tampere University
Master's Degree Programme in Electrical Engineering
November 2020
Examiners: Assoc. Prof. Sergey Andreev, Dr. Dmitri Moltchanov
Supervisors: Dr. Mikhail Gerasimenko, Assoc. Prof. Sergey Andreev

---

In the past few years, the use of smart devices and the amount of data traffic have been increasing significantly as more and more practical applications using wireless networks were being developed. Hence, machine-type communication (MTC) becomes an important use case for current and future wireless technologies. It covers a wide range of usage areas, for example, industrial automation, smart agriculture, and personal healthcare. This thesis focuses on the application of MTC for autonomous robotics, especially in maritime environments. To minimize the human's interaction on operation, the unmanned offshore system requires an inter-connectivity among the vehicles to exchange telemetry messages, sensor data and to stream surveillance video to a ground station. It leads to a demand for a wireless connection, which works without session interruptions, and provides high data rate, and covers a wide range. Hence, this thesis aims to develop a high-speed long-range communication solution for autonomous maritime operations. To achieve that purpose, a system of directional radio interfaces utilizing IEEE 802.11 Wi-Fi is designed and implemented on three core components of the offshore system: ground control, Unmanned Surface Vehicle, and Unmanned Aerial Vehicle. Each subsystem incorporates mechanical structures and motors, networking devices, and electrical components to form a functional communication solution. In addition, a beam-steering algorithm is developed and implemented for directional radio interfaces. Then, the system is tested in practice and the performance is evaluated in terms of throughput and received signal strength. Moreover, the results are compared with reference theoretical radio propagation models. Here, the details of the system implementation, appropriate tests, and analysis are summarized, evaluated, and discussed.

Keywords: Machine-Type Communication, autonomous offshore vehicles, wireless networks, beam-steering, directional antenna.

PREFACE

The research work reported in this thesis is the result of almost one year that I worked as a research assistant in W.I.N.T.E.R. research group in Tampere Univeristy, Finland. The thesis work is a part of the Autonomous and Collaborative Offshore Robotics (aCOLOR) project funded by the Technology Industries of Finland Centennial Foundation.

Firstly, I would like to express my sincere gratitude to my supervisor, Dr. Mikhail Gerasimenko, for his continuous support and detailed advice that benefited my motivation and knowledge. His guidance helped me in the course of conducting research and writing this thesis. My sincere thanks also go to my co-supervisor Assoc. Prof. Sergey Andreev for his patience and guidance. He helped in the beginning of the research assistant work and still supports me during the thesis writing process. Many thanks to Jani Urama and Dr. Alexander Pyattaev for being supportive. I would also like to thank the Unit of Automation Technology and Mechanical Engineering of Tampere University, especially Jose Villa Escusol, and Alamarin Jet Oy, for providing the necessary devices for the research.

I would like to extend my appreciation to all my friends in Finland and also in Vietnam for helping me in many ways. Special thanks I would like to give especially to my friends in Hervanta for bringing all the laughs and encouragement to me during my time at Tampere University.

Last but not least, I want to send my deepest thanks to my family and Phuong Doan for continuously supporting me through my hardest times. Thank you very much.

Contents

List of Figures

List of Tables

List of Programs

List of abbreviations

3D	Third Dimension.
3GPP	The 3rd Generation Partnership Project.
4G	Fourth Generation of Cellular Networks.
5G	Fifth Generation of Cellular Networks.
aCOLOR	Autonomous and Collaborative Offshore Robotics.
ADC	Analog-to-Digital Converter.
AP	Access Point.
AUV	Autonomous Underwater Vehicle.
BS	Base Station.
CPU	Central Processing Unit.
DC	Direct Current.
ERP	Effective Radiated Power.
GC	Ground Control.
GNC	Guidance, Navigation, and Control.
GPIO	General Purpose Input/Output.
GPS	Global Positioning System.
GTD	Theory of Diffraction.
H2H	Human-to-human Communication.
HD	High Definition.
IEEE	Institute of Electrical and Electronics Engineers.
IF	Intermediate Frequency.
IMT	International Mobile Telecommunication.
IoT	Internet of Things.
IP	Internet Protocol.
ITU	International Telecommunication Union.
LOS	Line Of Sight.
LTE	Long-Term Evolution.

M2M	Machine-to-machine Communication.
MIPS	Millions of instruction per second.
mmWave	millimeter Wave.
MTC	Machine-Type Communication.
nLOS	non Line Of Sight.
PoE	Power over Ethernet.
QoS	Quality of Service.
RAM	Random-access Memory.
RPM	Revolutions Per Minute.
RSS	Received Signal Strength.
RSSI	Received Signal Strength Indicator.
TCP	Transmission Control Protocol.
UAV	Unmanned Aerial Vehicle.
UPD	User Datagram Protocol.
USB	Universal Serial Bus.
USV	Unmanned Surface Vehicle.
UTD	Uniform Theory of Diffraction.
WLAN	Wireless Local Area Network.
WPAN	Wireless Personal Area Network.

1 Introduction

1.1 Motivation

In the past few years, we have witnessed significant growth in the use of International Mobile Telecommunications. As more and more smart devices with affordable price such as smartphones, tablets and home Internet-of-Things (IoT) devices along with the easy access to the Internet, the mobile data traffic faces a huge number of subscribers. International Telecommunication Union (ITU) predicts that the number Machine-type Communication (MTC) devices will be 7 billion by 2020 and will grow up to 97 billion by 2030 [1]. Besides the sky-rocket rise in numbers of devices, bandwidth demanding applications such as high definition video streaming and augmented/virtual reality are in development. Along with it, the introduction to low-latency applications such as healthcare will lead to a significant rise in data traffic capacity requirements [2].

Regarding the MTC usage, it covers a wide range of areas. The main focused use cases of this communication type include smart industry, agriculture and personal healthcare [3]. In factories, industrial automation depends on mission-critical MTC where it demands an ultra-reliable and low-latency connection [4]. The use cases extend to smart agriculture like intelligent irrigation based on surrounding conditions sensing [5] and to healthcare, for example, for personal wearable devices [6].

Another use case of MTC is for autonomous robotics. It utilizes the high speed and long range communication aspect of MTC since these unmanned moving machines require a high data rate wireless link [7]. Among all types of intelligent moving vehicles, the scope of this thesis concentrates on autonomous offshore systems. The goal of this system is to reduce human's interaction on maritime operation; hence, seeks for safe, effective and lower cost approach for monitoring and maintenance of maritime environment [8].

The autonomous maritime robotics rise demands on high data rate, latency and reliability [3]. However, the present network infrastructure and communication technologies cannot satisfy those demands. Thus, it is important to find out a solution and implement its prototype with current wireless communication standards to build a desired system. The designed system will be evaluated for its performance.

1.2 Objectives

The core objectives of the project are to research and to introduce a solution for unmanned offshore vehicles. A wireless communication system plays an important role for the purpose of inter-connectivity among the moving machines. In particular, it supports the use of telemetry, the transmission of sensors data and High Definition (HD) video streaming for monitoring and unmanned operation. The goal of this thesis work is to deploy and to test a radio network with high data rate and wide coverage for the maritime vehicles. As the trend goes for automation in transportation with MTC, implementing a prototype of a communication solution for unmanned offshore operation creates a huge opportunity for autonomous maritime ecosystem.

The solution proposed in this thesis utilizes an existing wireless technology which is IEEE 802.11 Wi-Fi[1]. We aim to implement a prototype of communication link among three components in the autonomous maritime system which are Unmanned Surface Vehicle (USV), Unmanned Aerial Vehicle (UAV) and ground control (GC). This will be the first step towards intelligent maritime operations. To satisfy the requirement of high data rate and wide coverage, directional antennas are equipped on the autonomous vehicles, that leads to the need in a beam-steering algorithm for these wireless devices. This method guarantees that the main lobes of directional antennas are aligned. Then, we evaluate the performance of the new system based on two metrics: throughput and signal strength level. In general, the main goals for this thesis are listed below:

- Implement a high-speed long-range communication system using IEEE 802.11 Wi-Fi standard for autonomous vehicles including USV, UAV and GC.
- Implement a beam-steering based on location data for directional antennas installed on moving machines.
- Conduct a measurement campaign to collect performance data of the system.
- Evaluate the practical results by comparing them with analytical models.

1.3 Scope and outlines of the thesis

This thesis consists of two main parts. Firstly, The design and implementation of wireless communication system for the ground control and moving machines are discussed. After that, the thesis focuses on the two testing scenarios and on the

[1]http://www.ieee802.org/11/

comparison of simulation and measurement results. The first scenario is Line-of-Sight communication between GC and USV. The second one is in non-LOS case where the UAV is deployed to act as a relay node. The detailed organization of the chapters is described as follows:

- Chapter 1 presents an overview on the topic under consideration. It discusses the motivation, the objectives and the structure of this thesis.
- Chapter 2 provides background knowledge on the concept of MTC, the current wireless network standards for MTC. It also discusses the definition of radio propagation models and how they contribute to the evaluation of the radio links. In addition, the performance metrics, which are throughput, received signal strength, latency, and reliability, are discussed in details.
- Chapter 3 describes prototyping the wireless communication system, which is a part of a project called Autonomous and Collaborative Offshore Robotics (aColor). This chapter focuses on designing and implementing of the telecommunication solution for three components: GC, USV and UAV. It includes system design, final mechanical and electrical design along with development for message exchange process and location based beam-steering algorithm.
- Chapter 4 discusses performed measurements and channel model simulation. It explains the channel models used for evaluation. This section describes the practical test scenarios and theirs results, then the evaluation is conducted using the comparison between real and simulated results.
- Chapter 5 summarizes the implementation process of the prototype and provides some future work proposals.

2 Background

This chapter covers technical background related to the thesis. In particular, Section 2.1 explains the definition of MTC. Section 2.2 presents some standard wireless networks which are used for MTCs. Section 2.3 demonstrates radio wave propagation modeling of the system, aiming to familiarize the reader with the theory of radio channel modeling, which will be used later on in this thesis. Section 2.4 explains the metrics used to evaluate the performance of the designed network, which consequently will be applied to assess the performed work at the end of the thesis.

2.1 Machine-type Communication

In the past few years, the usage of mobile communication and smart devices has developed significantly. This change led to a possibility of assessing the Internet everywhere at any time in almost every country, that brings on the growth of mobile data traffic. In the near future, this trend is supposed to skyrocket and will play a substantial role in every aspect of human life [9]. However, though the original purpose of mobile communication technologies is for human-to-human communication (H2H), although it also promotes the development of a machine-to-machine communication (M2M).

In fact, M2M, which is referred to as a direct communication between devices using either wired or wireless communication channel, have been modified to be called as MTC by 3GPP (The 3rd Generation Partnership Project) [10]. According to the 3GPP definition, MTC is the direct communication among autonomous nodes or through central servers allocated for MTC devices [11]. The main usage of MTC, both wired and wireless, can be ranged from smart industry such as factory automation, smart agriculture such as environmental sensing, to security surveillance cameras or healthcare applications [3].

At a first glance, the concept of MTC along with its basic requirements can be confused with the idea of Internet of Things (IoT). However, although sharing some similarities, the two concepts contain many critical differences. IoT, in simple terms, focuses on the combination of cloud services, connectivity analysis and communication technology, so that a smart environment including everyday embedded objects is enabled. These devices feature a network connectivity to improve its functionality and communication. Meanwhile, MTC is concentrating on the basis of connection between machines. In general, it can be seen that the IoT is actually a more all-encompassing term.

In brief, the concept of MTC is actually derived from M2M by 3GPP [10]. Its main focus is to reduce the part of human interaction on machine communication with a variety of applications. With two basic requirements it can be easily mistaken with IoT. However, both technologies, despite sharing many things, have many considerable differences. In fact, in recent years, researchers in the whole world become more interested in MTC as 5G is about to launch [12]; however, there are other wireless standards, that could be used as a basis for MTC [13].

2.2 Wireless networks for MTC

With the increasing trend of mobilizing every device nowadays, it could seem obvious that wired connectivity, which is the traditional way of networking, is gradually proven to be insufficient [14]. With a growing use of mobile devices, it has introduced new problems in both mobility and data traffic demand area to researchers. In general, every wireless network regardless the protocol always implies these two features [15]:

- *Mobility*: This is one of the distinguishing aspects of a wireless connection. It is allowing end-users to move freely without any limitations associated with infrastructure of the network, e.g. cables.
- *Flexibility*: This is the ability to support the mobility feature of wireless system in which devices will freely connect with the access point or base station. The capacity, coverage, security of the network access entities will be a matter to the connection of users. If three factors above can be satisfied, the system can be deployed without any restraints in environment and network performance. By achieving this feature, the network will reduce the difficulty of deployment and support costs.

The direction of development of wireless communications depends on the target application. In particular, MTC could be implemented using a number of different communication standards, providing different kinds of support for the purpose of the application. Among those categories, some of the most common ones are listed below:

- *IEEE 802.15 Bluetooth*: provides a close-range communication between two or more devices. Its applications are mostly utilized in Wireless Personal Area Network (WPAN) and IoT wearable devices.
- *IEEE 802.11 Wi-Fi*: a type of certification program licensed by Wi-Fi Alliance

that consists of all the vendors manufacturing products. They are based on Institute of Electrical and Electronics Engineers (IEEE) 802.11 standards[1] [16]. Since the first creation, Wi-Fi has gone through a lot of additions and modifications to improve the accessibility. For example, IEEE 8022.11n[2] and IEEE 802.11a[3] are both standards for the Wireless Local Area Network (WLAN). These technologies are two different modifications with different data rate, throughput and connectivity. In addition, Wi-Fi runs in an unlicensed spectrum using an access point (AP) as the network's local server. The AP will broadcast detectable control messages to other devices in order to create a WLAN network. Although being usually considered as an independent technology, Wi-Fi is only a brand name.

- *3GPP LTE*: this is another wireless technology targeting high speed mobile communication[4]. It has another name called "The fourth generation of broadband cellular networks" technology or 4G. This standard provides considerably faster connection than the third generation, while having significant lower latency. Besides that, 3GPP LTE also works in licensed spectrum in comparison with Wi-Fi.

- *Millimetre wave (mmWave)*: is a novel set of technologies working on mm-wavelength frequencies with tremendously fast data link rate enabled by utilizing wide bandwidth. Standards organizations like 3GPP and IEEE are trying to create the suitable protocols which will allow wireless communication operating in both licensed and unlicensed parts of the mmWave spectrum [17].

- *5G*: is the next generation of wireless communication technology providing a higher throughput and lower latency [18]. This is one the most attractive field for researcher to practice MTC since the bandwidth of 5G can support a massive MTC [13].

With various standards for wireless communications, we can choose a suitable one for the application of MTC based on the requirements of the system such as connection range, data transmission speed or energy consumption.

[1] http://www.ieee802.org/11/
[2] https://standards.ieee.org/standard/802_11n-2009.html
[3] https://standards.ieee.org/standard/802_11a-1999.html
[4] http://www.3gpp.org/technologies/keywords-acronyms/98-lte

2.3 Radio propagation modeling

To predict the behaviour of the wireless system, we need to characterise its response using the analytical radio propagation model. By taking into account the effects of terrain on the power density and Quality of Service (QoS), path loss model or radio propagation model is one of the key factors in analyzing the radio link performance for wireless communication systems [19].

A radio propagation model, sometimes called radio wave propagation model, is a mathematical formulation which aims to characterise the behaviour of the electromagnetic wave propagation in connection with frequency and distance assuming certain environments. This kind of model is often created to anticipate the responses of propagation for radio links with the same limitations. With the main aim of formalizing how radio waves are propagated, these models predict the channel path loss and define the transmitter coverage area. The models calculate the median path loss for a wireless link with the possibility of considering environment effects. Some typical factors which affect the radio channels are reflection, diffraction, scattering, refraction, noise and interference.

- *Reflection*: When an electromagnetic wave travels from one medium to another, it got reflected and partially transmitted [20]. In wireless communications, reflection is happening when the medium or the object which the signal intercepts is relatively larger than the wavelength of the signal [21]. The reflection coefficient of a material depends on the polarization, the incident angle and the frequency of the transmitted wave. For the relative conductivity value, it mainly depends on the frequency of the transmitted wave [22].

- *Diffraction*: When a transmitted radio wave intercepts a sharp edge, it is diffracted [21]. The effect could be observed as secondary wavelets propagating into a shadowed region [20]. Diffraction is an important phenomenon since it helps radio wave to propagate to curve surface, or behind an obstacle even though the signal strength in the shadowed region decreases dramatically. However, the diffracted field has adequate strength to produce useful received signal [22].

- *Scattering*: This is the spreading of the energy in all directions when a radio wave comes upon a rough surface [20]. Scattering theory often assumes that roughness of the surface is random. Many constructive or destructive interference may occur due to scattering and can have an impact on the received signal strength.

- *Refraction*: This is a phenomenon when a radio wave changes its direction

after encountering the lower atmospheric layer. The electromagnetic wave is bent due to various physical factors such as air pressure, temperature and humidity [23]. Among those, the moisture content above the water surface called ducts has a significant effect on radio wave propagation [24, 25]. It has been proven that the evaporation duct layer can increase the received signal strength for transmission with frequency above 3 GHz [26]. Hence, it is important to consider this effect for wireless communication links, especially for those occurring near a water surface.

- *Noise and Interference*: Noises and other disruptions can cause a significant effect to the communication link between the transmitter and receiver. To cancel that noise out, low-noise signal amplifiers are used on the receiver side of the system. The transmission quality depends on the Signal-to-Noise Ratio (SNR). There are several types of noises and interference which can cause the disruptions such as thermal noise, man-made noise, or atmospheric noise.

As with all experimental models, radio propagation models do not exactly indicate the characteristics of a link, rather, they predict the most likely one depeding on the considered conditions.

The most basic model is free space propagation model. It describes the ideal condition between transmitting and receiving antenna where only line-of-sight link exists and no other obstacles or structures are around. Therefore, we can only apply this model to practical cases in open space where the radio link is LOS and there are no obstacles nearby. For non-ideal scenarios, there are various approaches to characterize the radio channels. These modelling methods can be divided into 3 categories [27]:

- *Ray tracing propagation models*: In practice, there are terrain surfaces and infrastructure objects from which the radio can be reflected or refracted. By analyzing the geometry of the scenario and the multipath trajectory of the signal, these methods can give estimation of the channel model. This method is common for environments with limited surfaces and terrestrial objects. Two-ray model is one of the well-known models which is using this approach. It assumes that there are two rays: one is direct and the other is reflected from ground or water surface.

- *Deterministic models*: These methods determine the signal power considering the path profiles which includes environmental factors between the transmitter and the receiver by utilizing fundamental equations of electromagnetic theory. Deterministic models mostly use ray optical theory and some methods like

Geometrical Theory of Diffraction (GTD) and Uniform Theory of Diffraction (UTD). Generally, these kinds of approaches take into account the combination of direct ray between devices and other rays which are reflected, diffracted and scattered. The number of considered paths determines the complexity building the model. Moreover, the more complex models are, the more accurate results they demonstrate. However, it usually requires more computational power.

- *Empirical models*: In some cases, the knowledge of the environmental profile is insufficient, so it is not possible to apply deterministic models. Hence, this type of model is built based on practical measurement results obtained from measurement campaigns. Some significant empirical models are Okumura-Hata model and Walfisch-Ikegami model [28]. Since these models are based on specific scenarios, their estimation accuracy also depends on environmental parameters. For example, Okmura-Hata model is suitable for urban and suburban areas while Walfisch-Ikegami method is more accurate when applied to dense city environment [28]. Empirical models use simple equations and thus require less computation compared to deterministic ones. However, they provide less accurate results and are restricted to specific environments and scenarios.

2.4 Performance metrics

One of the objectives of this thesis is to investigate the performance of the radio link in scenarios with mobile autonomous vehicles. The performance metrics includes throughput, received signal strength, latency and reliability, which are used to evaluate the communication system. These metrics are discussed in this section.

2.4.1 Throughput

In general, throughput describes the operation processed per unit time such as jobs per day, millions of instruction per second (MIPS), bits per second, etc [29, 30]. In communication context, throughput refers to the rate of successfully delivering messages through a communication channel between two networking terminals [31, 32]. The data rate is the rate at which the packets are transmitted and it shows possible achievable throughput if whole channel bandwidth is utilized; meanwhile, throughput indicates the general transmission rate taking into account the higher layer overheads, interference or protocol inefficiencies, etc [33, 32, 31]. We use this metric to evaluate the amount of packets transferring between two devices installed on the autonomous vehicles. In particular, throughput of the Transmission Control Protocol (TCP) data packets is investigated in the result section.

2.4.2 Received Signal Strength

In communication systems, received signal strength (RSS) is a measurement of how much power present in the signal of reception. RSS is often unknown to a receiving user's device. However, as signal strength can fluctuate greatly and impact on the functionality of the wireless network, the measurement is often made available to users in many IEEE 802.11 devices.

The derivation of RSS is usually preformed at the intermediate frequency (IF) stage before the IF amplifier. In direct conversion systems which exclude the IF stage (zero-IF), the received signal strength is deduced in the signal chain of the baseband prior to the baseband amplifier. RSS value is usually a DC analog level and it may also be collected by an analog-to-digital converter (ADC) [34].

The RSS is measured in decibels milliwatts (dBm) and the received signal level for communication devices is ranging between 0 dBm as maximum (theoretically) achievable value and sensitivity threshold (e.g. -110 dBm) as very poor signal. RSS level is influenced by the quality and quantity of obstacles from transmitter to receiver, along with how far devices are separated from each other. This factor is characterised as path loss from surrounding environment. The RSS can be improved by increasing antenna gain or increasing transmitting power to compensate for the propagation loss. The formula 2.1 is used for calculating received signal strength indicator [35]:

$$RSSI = P_{tx} + G_{tx} - PL + G_{rx}, \tag{2.1}$$

where
RSS: received signal strength [dBm]
P_{tx}: transmission power [dBm]
G_{tx}: transmitter antenna gain [dBi]
PL: propagation loss or path loss [dB]
G_{rx}: receiver antenna gain [dBi]

2.4.3 Latency and reliability

There are other performance metrics which we did investigate in our work, from which the most common are latency and reliability. However, they are also important for evaluating the wireless network performance. Thus, we will briefly describe them in this section.

Latency defines how long it takes for a packet to travel from the protocol layer of the source to the same layer at the destination device [36]. In wireless networks, the latency is defined as the sum of four components: propagation time, transmission time, queuing time and processing delay [37]. Propagation time is the time between a packet or a bit is sent on PHY layer of transmitter and received on PHY layer of destination. The transmission time also takes into account the lags of the inter-layer processing of the packet. The queuing time is the amount of time which a bit must wait before being sent and the processing delay is the time for the network device to process the messages.

Before mentioning the reliability term, we briefly introduce the packet loss definition. A packet is considered lost when it fails to reach it destination [38]. It usually happens due to errors in wireless data transmission or traffic congestion. Then, reliability is determined by calculating the probability of lost packet which can not be delivered to the destination within a certain latency constraint [18]. The fulfillment of this criterion guaranties the packet delivery in a particular time window.

3 Communication system for autonomous offshore vehicles

This chapter describes architecture design and implementation of the communication system for Autonomous and Collaborative Offshore Robotics (aCOLOR) project[1]. Here, we focus on simulation details of applicable propagation loss models and description of GC, USV, and UAV subsystems implementation.

3.1 State of the Project

The main goal of aCOLOR is to build up an essential methodology and to implement a prototype for an autonomous robotic system working in offshore environment which combines three elements: water surface, underwater and air. This multi-component system includes three core vehicles which are Unmanned Surface Vehicle (USV), Unmanned Aerial Vehicle (UAV) and an Autonomous Underwater Vehicle (AUV). Thus, the project proposes associate innovative approach for useful offshore intervention tasks in telecommunications, intelligent obstacle detection, and path designing [39]. This becomes more challenging when a network of diverse autonomous vehicles must co-operate to work as a unified system to achieve defined tasks. Therefore, the aColor project requires collaboration work among various fields of research main of which are mechatronics, machine learning and wireless communications [40].

One of the essential features of the unmanned maritime vehicles are the Guidance, Navigation, and Control (GNC) systems which are used for path following and obstacle avoidance [40]. In this project, the line-of-sight (LOS) path algorithm for straight-line has been developed and implemented for path planning and collision preventing as a GNC method for the autonomous moving vessel [41]. Besides that, the use of surveillance camera for intelligent observation and detection of objects on water surface is the focused research topic of machine learning side. The first step to achieve the objective is to recognize the water surface. Hence, a water segmentation algorithm has been studied and deployed during the first part of the [41]. For the telecommunication features, to support the continuous and high-speed communication among the unmanned vehicles, a prototype of directional radio link system has been built between the ground control and the USV [42].

[1] https://techfinland100.fi/mita-rahoitamme/tutkimus/tulevaisuuden-tekijat/autonomous-and-collaborative-offshore-robotics-acolor/

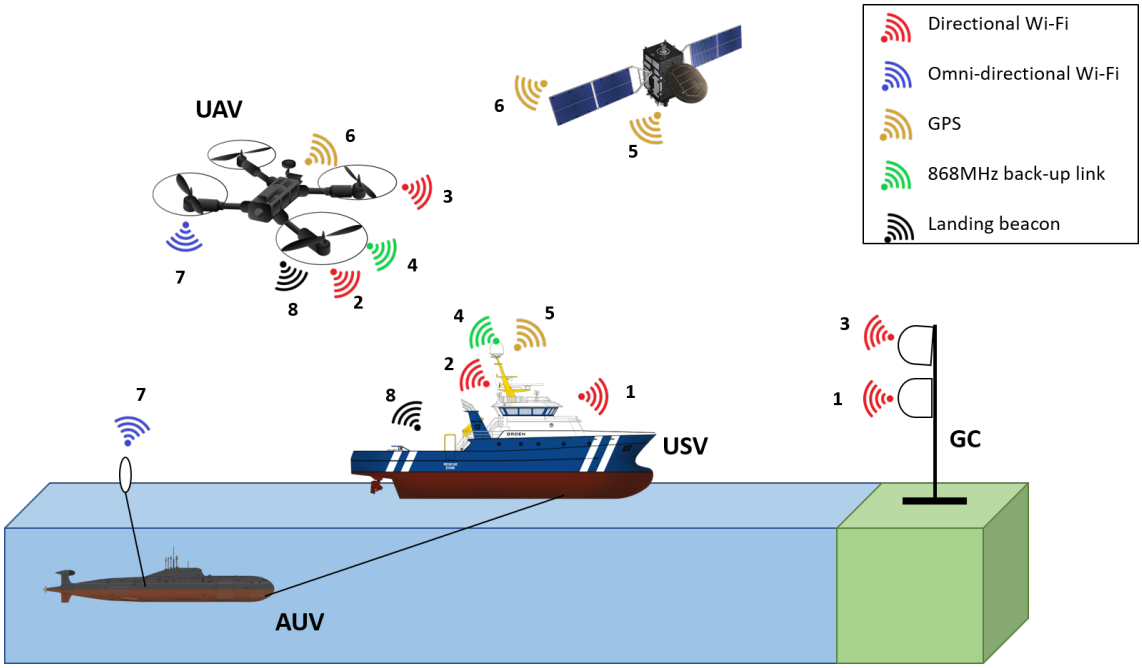

Figure 3.1 *General communication system for aCOLOR. The radio links are: 1. GC-USV directional Wi-Fi, 2. USV-UAV directional Wi-Fi, 3. GC-UAV directional Wi-Fi, 4. USV-UAV back-up link, 5. USV GPS link to satellite, 6. UAV GPS link to satellite, 7. USV-AUV non-directional Wi-Fi, 8. Beacon for UAV landing.*

The work in this thesis concentrates on the communication aspects. The major goal is to deploy and test long-range high-speed connections among system's mobile components to support various cooperative intelligent tasks without any discontinuity. The general communication architecture is illustrated in Figure 3.1.

This thesis continues the study of Zeinab. et al [42] in order to enable relay mode between GC and USV via UAV. Our system utilizes Wi-Fi 802.11ac (5 GHz bands) technology. Thus, it covers following tasks:

- Modify location-based beam-steering algorithm to operate with new mechanical components.
- Enable the radio links between GC-UAV and UAV-USV for establishing relay connection between GC and USV in nLOS scenarios and for extending the coverage of the offshore system.
- Simulate propagation loss and evaluate system performance by comparing with theoretical models.

3.2 Communication modes

The communication system between Ground Control station and Unmanned Surface Vessels implies two modes of operation: direct communication between GC and USV and relayed link between GC and USV via UAV. When the antennas on the ground control and the moving vessel still have the line of sight of each other, the system works utilizing direct communication mode. If the LOS is lost, the autonomous drone will be deployed from the water-surface vehicle. It will act as a relay node between the ground station and the boat. The USV and UAV each carries one directional antenna and one omni-directional antenna while GC is equipped with one directional antenna. The overview of this wireless system is presented in Figure 3.2.

3.3 System architecture

To enable the above mentioned modes of operations, USV, GC and UAV communication modules should be equipped with long-range high-throughput communication units. Long-range aspect could be enabled with dynamic steering of directional antennas. Each module combines various mechanical, networking and electrical components to feature the antenna steering capability. The design of the communication unit varies depending on the vehicle on which it is installed.

Regarding the layout of the system on the USV, it consists of a single-board computer, a motion sensor, two servo motors and a servo controller installed on the compound plate together with the directional antenna. These two servo motors are responsible for the vertical and horizontal steering of the antenna. For horizontal beam-steering of the USV antenna, the positioning data is collected from a GPS compass module by the USV main computer using ROS[2]. After that, this GPS signal is sent to the single-board computer via Ethernet. By assuming that the location of the GC is fixed, this computer calculates the steering angle by using the positions of the boat and ground station and then sends a control signal in the ROS format to the servo controller. The controller then activates a servo motor to rotate the USV antenna towards the GC station. When two antennas are connected through a Wi-Fi link, the USV's GPS coordinates will be sent to the ground system, which then will be collected by the controller board in GC. The GC steering system also includes a DC motor, a motor driver and a servo motor, and controls the DC motor to horizontally steer the antenna to the direction of the autonomous boat.

Both the antenna system on USV and GC have the capability of rotating vertically.

[2]Robot Operating System, https://www.ros.org/

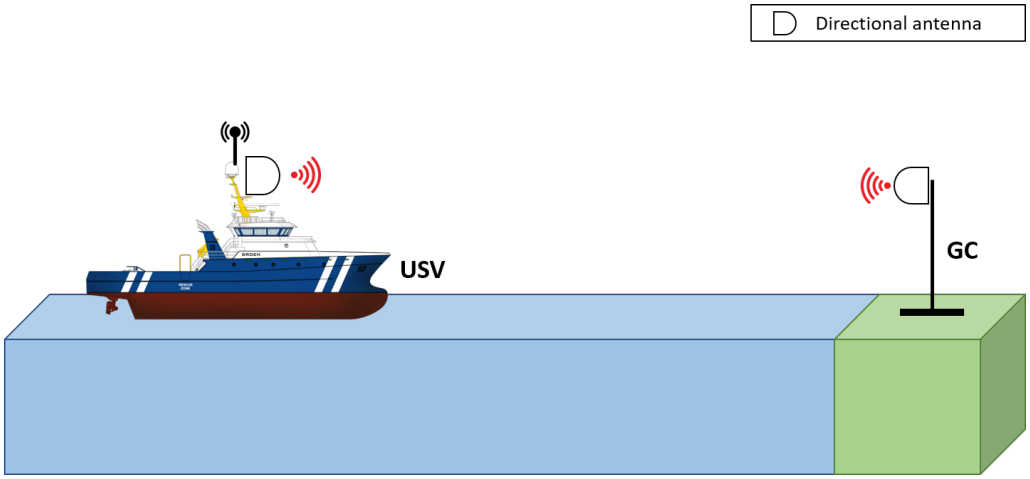

(a) Direct mode

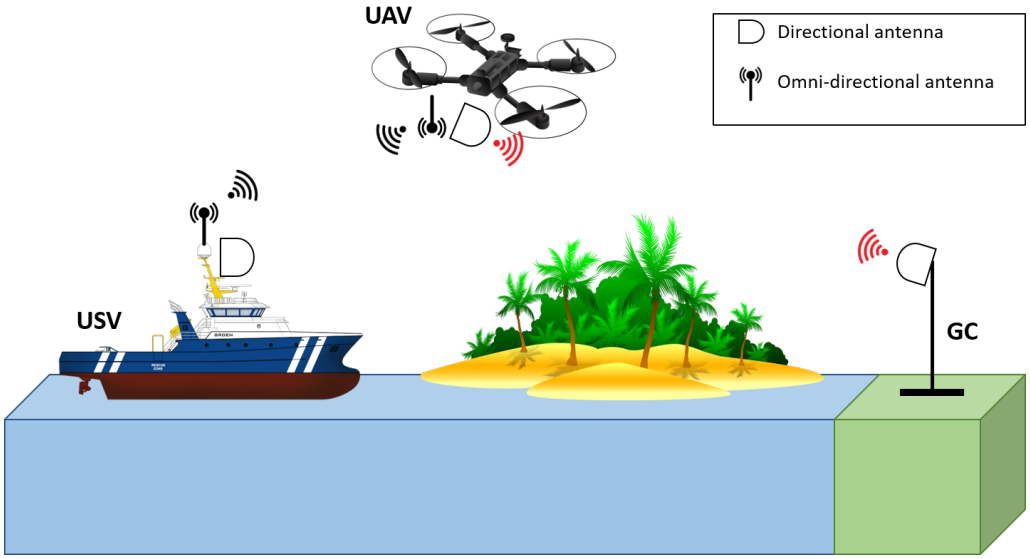

(b) Relay mode

Figure 3.2 *Two wireless communication modes*

Since the boat is floating on water, the tilting angle of the antenna may vary. To solve this, a 6-axis sensor is utilized to estimate the compensated vertical angle. The embedded computer will control the other servo to rotate the antenna in order to keep it stable against the waves. The servo motor in the GC system steers the antenna towards the flying UAV in case when the system works in the "relaying" mode.

In the case of nLOS, a UAV could be deployed to establish a relay link. The UAV steering system includes an embedded computer and a servo motor. The computer receives GPS coordinates, including latitude, longitude and altitude, to calculate the tilting angle. Then, it controls the servo to steer the antenna vertically. For

horizontal rotation, we utilize the yaw-control capabilities of the drone. It is keeping its heading towards a constant direction, which is our ground control station in this case. All the subsystems have a separate power regulator so that it can deliver a suitable power to each component.

Figure 3.3 and 3.4 show the layout of the design concept for USV, GC and UAV system, respectively.

3.4 Final design

This section presents the chosen devices and components for the system. The mechanical parts are designed and built in collaboration with the Unit of Automation Technology and Mechanical Engineering of Tampere University. The electrical parts are designed by the Unit of Electrical Engineering.

3.4.1 Mechanical implementation

For the mechanical frames of the antennas on the USV and GC side, they have been already created from previous phase of the project ([42]). In the current state, the USV communication system got some modifications to improve its resistance against the wind and to increase the precision of rotation as shown in Figure 3.5 (a). The two brackets holding the antenna were made from aluminum so that it could prevent the antenna from swinging when the wind is strong or the autonomous boat is moving at high speed. For the vertical rotation, two gears were placed on the bracket. One was connected to the servo motor through a shaft and the other was installed on the shaft of the antenna. A belt linked those two gears to transmit the rotary motion from the servo motor to the antenna. In this state, we used two ROBOTIS Dynamixel AX-12 servo motors[3] for both horizontal and vertical rotation of the boat antenna. The AX-12 servo features the tracking capabilities of its speed, temperature, shaft position, voltage, and load. The shaft position can be maintained and modified accordingly to each individual servo thanks to the control algorithm on the AX-12 actuator. It allows controlling the motor's response in terms of speed and strength. The servo's built-in microcontroller manages all of the sensors and position control. The servo produces high stall torque of 1.5 N·m and high no-load speed of 60 RPM, which are suitable for beam-steering rotation.

The directional antenna on UAV was installed to a carbon-fiber platform. The design of this frame followed the structure of the drone so that we could mount the system to the flying vehicle as shown in Figure 3.5(b). This mounting platform

[3]http://emanual.robotis.com/docs/en/dxl/ax/ax-12a/

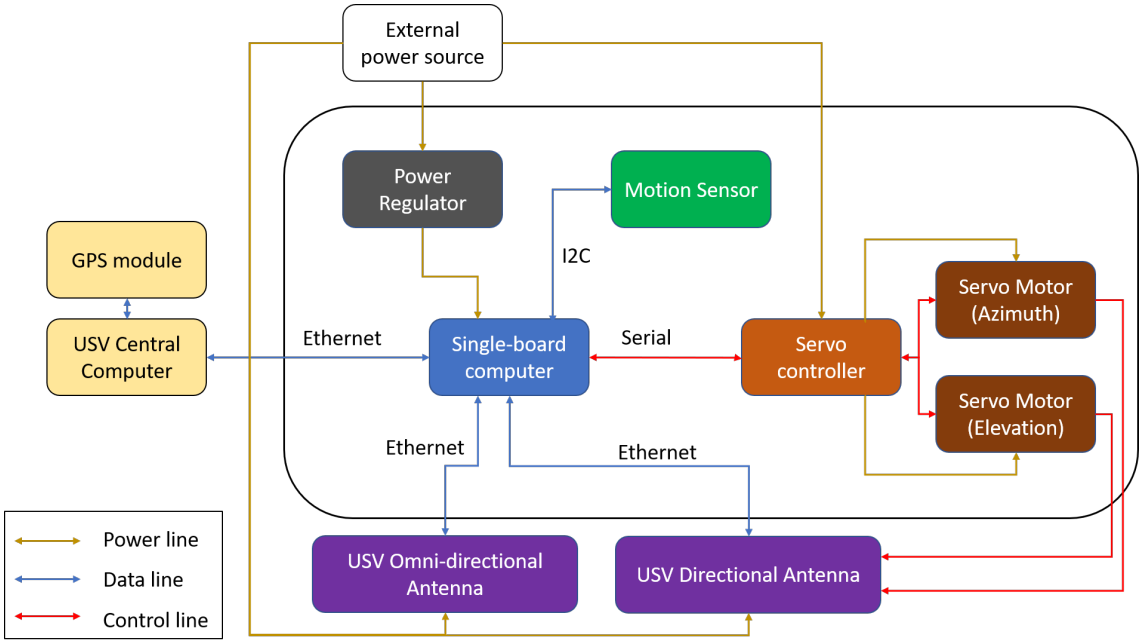

(a) Design concept for system on the USV

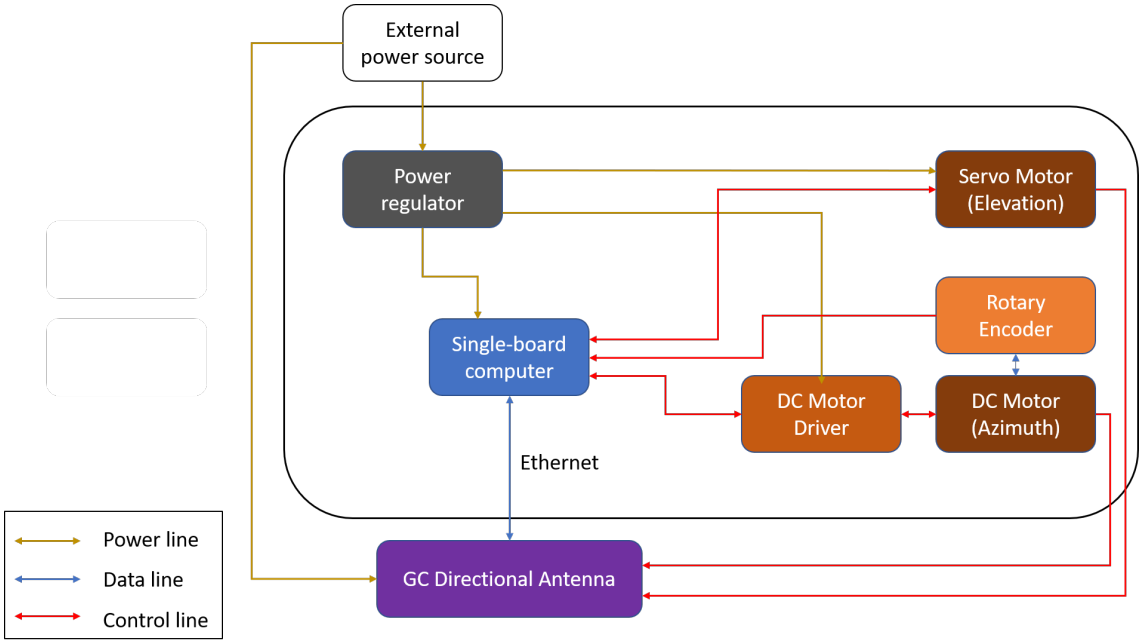

(b) Design concept for system on the GC

Figure 3.3 *System design concept layout for USV and GC*

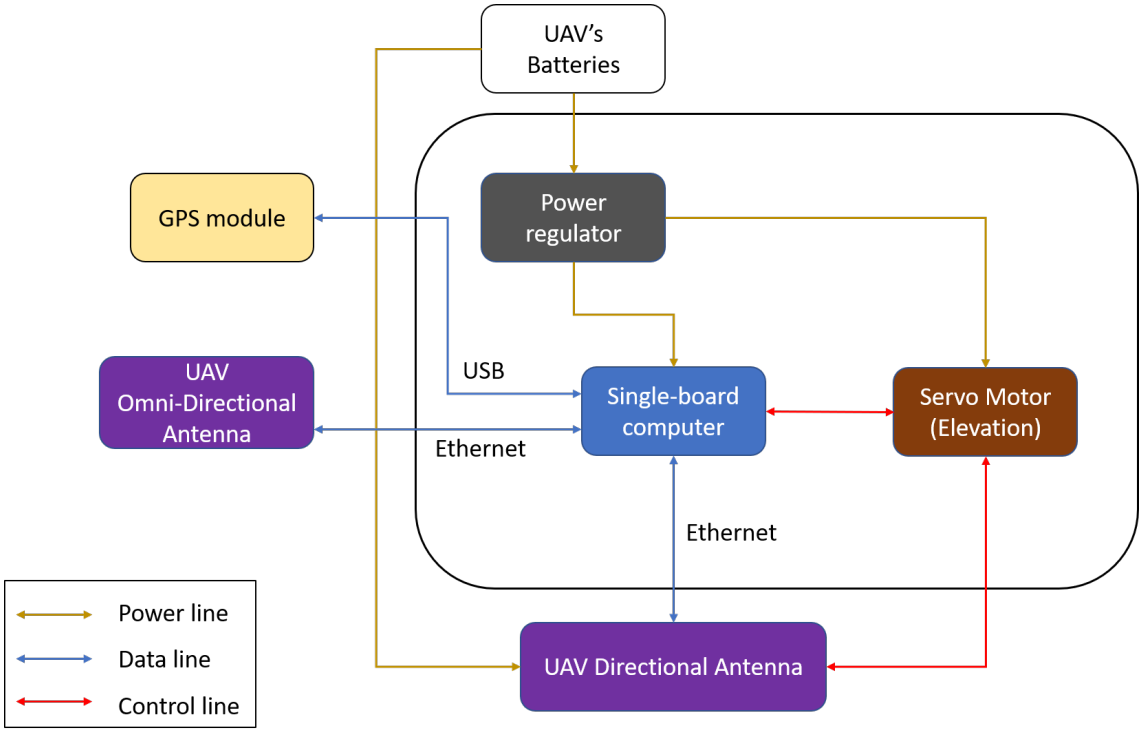

Figure 3.4 *System design concept layout for UAV*

consists of several plates and has enough space to place other electrical devices on it. The brackets holding the antenna and the gears were 3D printed. The servo motor shaft connected to one gear and the antenna was installed to the adjacent gear, which enabled the vertical rotation. Figure 3.5 shows the final mechanical design for the directional antenna on USV and UAV, respectively.

3.4.2 Networking devices

Antenna

For the wireless interfaces on USV and GC, our selection is MikroTik DynaDish 5[4], which supports new Wi-Fi IEEE 802.11a/n/ac (5 GHz) standard. This product is typically designed to establish a reliable point-to-point connection. Regarding the system on UAV, the devices have to be small-sized and light-weighted. Hence, the compact MikroTik SXT 5 ac is a suitable selection[5]. It utilizes the same communication standard as DynaDish 5; however, the SXT 5 model comes in a small size of 140x140x56 mm and a weight of only 265g. All the chosen MikroTik devices offer Gigabit Ethernet and are compatible with Power over Ethernet (PoE).

[4]https://mikrotik.com/product/RBDynaDishG-5HacDr3
[5]https://mikrotik.com/product/RBSXTG-5HPacDr2

(a) Final mechanical structure for USV's directional antenna

(b) Final mechanical design for mounting platform of UAV's directional antenna

Figure 3.5 *The final mechanical design of two antennas on USV and UAV*

Besides those, as mentioned in Section 3.3, MikroTik GrooveA 52 a [6] omni-directional antennas were installed in our system. The interfaces are using the same standard for wireless communication as the equipment above, and these devices come with a Dual Band 2.4/5 GHz Omni-directional antenna with the gain of 6 dBi for 2.4 GHz and 8 dBi for 5 GHz. The interface installed on a UAV side is TECHKEY USB 3.0 Wi-Fi Dongle[7]. It is a compact device with a 5 dBi antenna, which can offer up to 867 Mbps in Wi-Fi IEEE 802.11ac. It uses USB 3.0 as an interface to the controller board on the UAV.

Router

To connect all the devices on USV and GC side, two routers were utilized on each side. The core requirements for the routers are to provide Gigabit Ethernet and support PoE for connected devices. Since the MikroTik hEX PoE router[8] was installed and tested during the previous stage of the project, we decided to keep it.

[6]https://mikrotik.com/product/RBGrooveGA-52HPacn

[7]https://www.amazon.com/Adapter-1200Mbps-TECHKEY-Wireless-Network-300Mbps/dp/B07J65G9DD

[8]https://mikrotik.com/product/RB960PGS

Table 3.1 *Hardware specification of the Beaglebone Green board*

Feature	Value
Processor	AM335x 1 GHz ARMR Cortex-A8
RAM	512 MB DDR3
On-board storage	4 GB eMMC
Accelerator support	NEON floating-point and 3D graphics accelerator
Micro USB	1, for Powering and data communication
USB	1, for Hosting
GPIO	2 x 46 pin headers
Networking	1 Ethernet port
Operating temperuate	0 - 75 degree Celsius

3.4.3 Electrical components

Controller

The single board computers on both USV and GC side were Beaglebone green boards[9]. They were responsible for exchanging GPS messages, running beam steering algorithm and executing measurement scripts. Table 3.1 shows the hardware specification of the embedded computer.

For the UAV system, we used the Udoo X86 ULTRA version[10] single board computer. One task of the controller on the aerial vehicle is forwarding the network packets in relay mode. The Mikrotik SXT ac antenna and the Wi-Fi USB dongle would be respectively connected to the Ethernet port and USB port of this board. We chose Udoo X86 since it has a Gigabit Ethernet network interface and USB 3.0 to provide high data transfer rate. In addition, the chosen embedded board is compatible with Arduino™ 101 platform so it can control the servo motor using Arduino software. Besides those, this board has a powerful hardware which can be utilized for other autonomous tasks such as video processing. The technical specification of the board is presented in Table 3.2

Another controller used in the system was the Arbotix-M Robocontroller[11]. This robot controller is an advanced control solution for DYNAMIXEL servos and other high-accuracy robotic actuators. It incorporates a robust AVR microcontroller, a wireless interface, dual motor drivers, and 3-pin headers for hobby servos with digital

[9]https://beagleboard.org/green
[10]https://www.udoo.org/docs-x86/Introduction/Introduction.html
[11]https://www.interbotix.com/arbotix-robocontroller

Table 3.2 *Hardware specification of the Udoo X86*

Feature	Value
CPU	Intel® Pentium N3710 up to 2.56 GHz
GPU	Intel® HD Graphics
RAM	8 GB DDR3L Dual Channe
Video interfaces	1x HDMI 1.4 (CEC), 2x Mini DisplayPort ++
On-board storage	32 GB eMMC soldered on-board
Networking	1x Gigabit Ethernet LAN interface 1x M.2 Key E slot for optional Wireless Module
Audio interfaces	HD Audio Codec ALC283CG Microphone + Headphone Combo Connector (TRRS) Pre-amplified stereo speaker output,S/PDIF output
USB	3x USB 3.0 type-A sockets
Other interfaces	2x HSUART ports, 2x I2C interface, 1x SDIO interface 1x LPC interface
Platform compability	Arduino™ 101-Compatible through standard Arduino™ Pins layout, compatible with Arduino™ shields

and analog I/O. The Arbotix-M Robocontroller is for controlling two newly installed Dynamixel AX-12 servo motors.

Sensors

On the USV system, an Adafruit LSM9DS0[12] sensor was installed. This component incorporates 3-axis accelerometer, gyroscope and magnetometer. We used this sensor to detect the tilting of the directional antenna on the boat caused by moving on water waves. The Beaglebone board calculates the tilting angle, based on data collected by the sensor, and then rotates the antenna vertically to compensate the tilting. Program 1 (Python) in Appendix A shows the calculation of the vertical angle for the directional antenna on the water-surface vehicle. In the code, we were using *numpy* library for mathematical functions and the LSM9DS0 library for the sensor data recording. The input parameter to this function was the current horizontal angle of the antenna. Then, the pitch and roll values of the boat were read from the LSM9DS0 sensor and were used to define the plane in which antenna were positioned. The function *array()* creates an array of values, describing the plane. After that, we formed a vector from the rotation angle values of the antenna. Then, the projection, which told where the antenna was pointing in the xyz-plane, was

[12]https://www.adafruit.com/product/2021

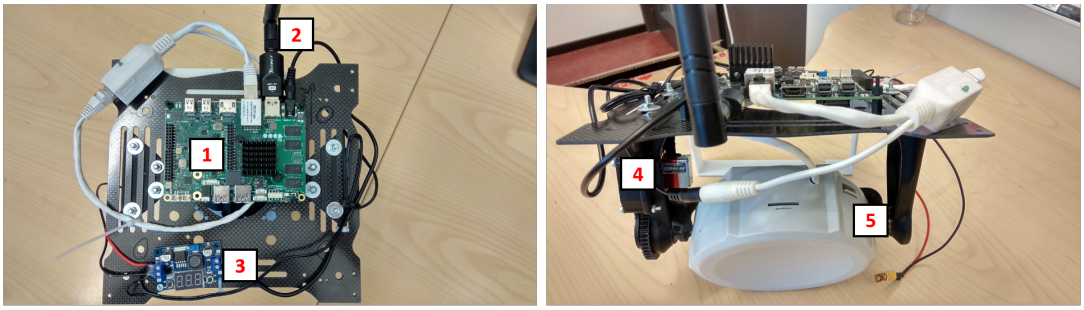

Figure 3.6 *Components location for the UAV communication system*

calculated. The *dot()* and *cross()* are dot-product and cross-product functions. The tilting angle was the angle between that vector and the defined plane in the xyz-coordinate which we had built. After horizontal angle is calculated, the antenna should be steered vertically against the calculated angle above to compensate the boat plane tilting.

Power

The supply power input varies for all the devices of the systems. Thus, it is necessary to install different power regulators for each equipment piece. For the USV system, the power was supplied from the ship accumulator and it was connected to the voltage regulators in the communication module of the moving vessel. The components on UAV were provided with the power from the drone's battery. In order to supply the appropriate power for different devices, we need to have an overview on the input power requirements of each component. Table 3.3 shows the voltage input for the devices used in the system.

For the ground control and unmanned surface vessel, the system has not had changes in components except the installment of AX-12 servos and Arbotix-M Robocontroller as shown in Figure 3.5(a). The final electrical design of the UAV is presented in Figure 3.6

3.5 GPS and control messages exchange methods

As mentioned in Section3.3, the single-board computer on each vehicle is responsible for running beam steering algorithm. It requires the location data to calculate the rotation angle and then sends commands to the desired motor. Hence, we designed a method for transferring GPS coordinates and controlling message among the devices in the system. Figure 3.7 shows diagram of the data and control message exchange steps between USV and GC sides.

Table 3.3 *List of the components used in the system and their input voltage*

Category	Item	Model	Quantity	Supply voltage [V]
Mechanical components	GC Servo motor	HS-805BB	1	4.6-6.0
	UAV Servo motor	TGY 306G-HV	1	4.8/6.0/7.2
	USV Servo motor	Dynamixel AX-12	2	12
Networking components	Directional antenna	MikroTik DynaDish 5	2	11-60
	Compact Directional antenna	MikroTik SXT 5ac	1	15-60
	Omni-directional antenna	MikroTik GrooveA 52	1	9-30
	Router	MikroTik hEX PoE	1	12-57
Electrical components	USV and GC controller	Beaglebone Green	2	5
	UAV controller	Udoo X86	1	12
	Servo controller	Arbotix-M	1	11-12
	DC motor driver	POLOLU-713	1	2.7-5.5
	Motion sensor	Adafruit LSM9DS0	1	2.4-3.6

First, since the ground control was placed at a fixed location, we set the GPS coordinates of GC to the controller on USV. Before the boat started running, the single-board computer on the USV collected its current location from the GPS compass using ROS messages. The controller calculated the rotation angle from the coordinates of the boat and the ground controller. Then, it sent the command to the servo motor so that the USV directional antenna was pointing towards the GC. As the two antennas got aligned, the USV controller transferred the location data of the boat to the GC side. These two embedded computers used two antennas to exchange these messages through UDP. When the GC controller acquired the GPS data of the boat, it calculated and sent rotation command in pulse-width modulated signal to the DC motor. These steps were repeated as the water-surface vehicle was travelling along its route.

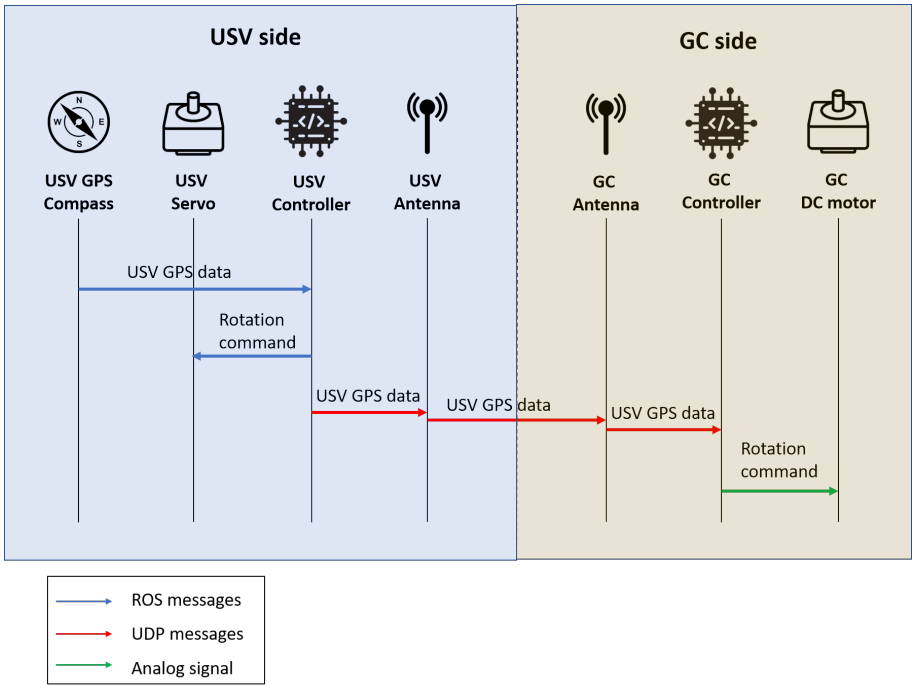

Figure 3.7 *Signaling message exchange steps between the devices*

3.6 Location-based beam-steering algorithm

In order to align the beams of the directional antennas in the system, an algorithm for beam-steering based on devices' location was developed. It was implemented in the embedded computer on the system of each vehicle. The program included two parts: calculating the beam-steering angle and sending control commands.

Assuming that the single-board computers had collected the positions of the moving vehicle and the ground control, they calculated the angle between the line connecting these two points and global coordinates axes. We also took into account the curve of the Earth's surface due to long distances of the run route. Then, the formula for calculating the angle difference, or the bearing angle, between two sets of coordinate points (ϕ_1, λ_1) and (ϕ_2, λ_2), which was obtained from [43], is given by :

$$Angle = \arctan\left(\frac{\sin\Delta\phi\cos\lambda_2}{\cos\phi_1\sin\lambda_2 - \sin\lambda_1\cos\lambda_2\cos\Delta\phi}\right). \tag{3.1}$$

The latitudes and longitudes in the formula above must be in radian units. After obtaining the desired angle, the board sent a ROS message with the angle value to the servo controller. The rotation mechanism and connection of the servo motors were implemented by Unit of Automation Technology and Mechanical Engineer-

ing of Tampere University. The pseudo code of the algorithm in Python language syntax, which is obtained from prior work of Zeinab. et al [42], is presented in Program 3.1. In the beginning of the loop, the script calculated the angle between GC and USV, which was the variable *angle*, using Equation 3.1. The function *atan2()* implied the calculation of the arc-tangent of the ratio of its two parameters. The coordinate values should be in radians, in order to do that, the function *radians()* was applied to those values. The result from above was the angle difference between the ground control and the moving vessel. Since the boat had its own heading, we needed to consider its value to know the rotation angle for the servo motor. After acknowledging the *heading* and the angle position of the servo *servo.last_pan_angle*, the script calculated the angle for the servo to rotate. Finally, the function *servo.rotate_pan_to_angle* sent the commands with desired rotation angles to the servo motors.

Program 3.1 *The beam-steering algorithm [42]*

```
lon[0] = USV longitude;
lat[0] = USV latitude;
lon[1] = GC longitude;
lat[1] = GC latitude;
while True:
    if heading!=0:
        delta_lon = lon[1] - lon[0]
        angle = degrees(atan2(sin(radians(delta_lon)) *
            cos(radians(lat[1])),
            cos(radians(lat[0])) *
            sin(radians(lat[1])) -
            sin(radians(lat[0])) *
            cos(radians(lat[1])) *
            cos(radians(delta_lon))))
        heading_diff = heading -
            current_heading
        angle_diff = angle-servo.last_pan_angle -
            heading_diff
        angle_diff = sign(angle_diff)*
            (abs(angle_diff) % 360)
        current_heading = heading
        servo.rotate_pan_to_position(angle-heading_diff)
```

Using the same algorithm, we could set the drone's yaw in such order, that the installed antenna was horizontally aligned with the GC. Hence, we did not need to implement a separate mechanism for UAV antenna rotation in horizontal plane. For the tilting of the antennas on the aerial vehicle and GC (GC-UAV connection), we used the Formula 3.2 obtained from [44] to calculate the elevation angle between two points with elevation $elev1$ and $elev2$ above the ground:

$$Elevation\ angle = \left(\frac{180}{\pi}\right)\left(\frac{elev2 - elev1}{d} - \frac{d}{2R}\right), \tag{3.2}$$

where R is the Earth's radius and d is the distance between two points, which are calculated by Haversine formula [44]:

$$d = 2r\ sin^{-1}\left(\sqrt{sin^2\left(\frac{lat2 - lat1}{2}\right) + cos(lat1)\,cos(lat2)\,sin^2\left(\frac{lon2 - lon1}{2}\right)}\right). \tag{3.3}$$

For the code implementation, we just need to replace the horizontal angle calculation part of the Program 3.1 with the two formulas above to find the tilting for the directional antenna on the UAV and GC.

4 Experimental results and performance evaluation

This chapter presents the results of measurement campaign done during summer 2019, which includes two different scenarios, described in chapter 3. Once the measured values have been recorded, the performance of the system is evaluated based on channel model simulation.

4.1 Path loss models

The simulation for propagation loss is based on existed channel model. Since our system consists of direct mode and relay mode, the estimation focuses on two possible scenarios of the practical radio links which are GC-USV and GC-UAV-USV. The first model could be charaterized as Line-of-Sight communication in the near water-surface environment, and the other is based on free space propagation mode. Besides that, wireless devices used in this system are built upon Wi-Fi 802.11ac; thus, the selected channel models are adjusted for 5 GHz frequency bands.

The simulation-based analysis of above-mentioned models is done using Matlab software[1]. In radio-wave propagation models, some constant parameters have to be chosen to match with the real system while frequency and distance are variables. As mentioned above, our interfaces are working on 5 GHz frequency band; hence, by varying the distance, we can use Matlab to calculate the path loss and then plot the RSS.

4.1.1 Near water-surface LOS channel model

To characterize the propagation over water surface, we used the channel model from the study of Lee. et al [45] which proposes a combination of 2-ray and 3-ray models. The authors of the paper conducted measurements with a distance of up to 10 km. Their analysis shows that the received signal strength agrees well with the prediction from 2-ray model for close range (before the break point d_{break}). However, as the transmission distance increases farther than d_{break}, its estimation ability becomes less precise. Therefore, 3-ray model can improve the precision by taking into account the ducting effect.

When the transmitted radio-wave propagates directly towards the receiver and reflects from the water surface the propagation loss can be estimated by a 2-ray path

[1] https://www.mathworks.com/products/matlab.html

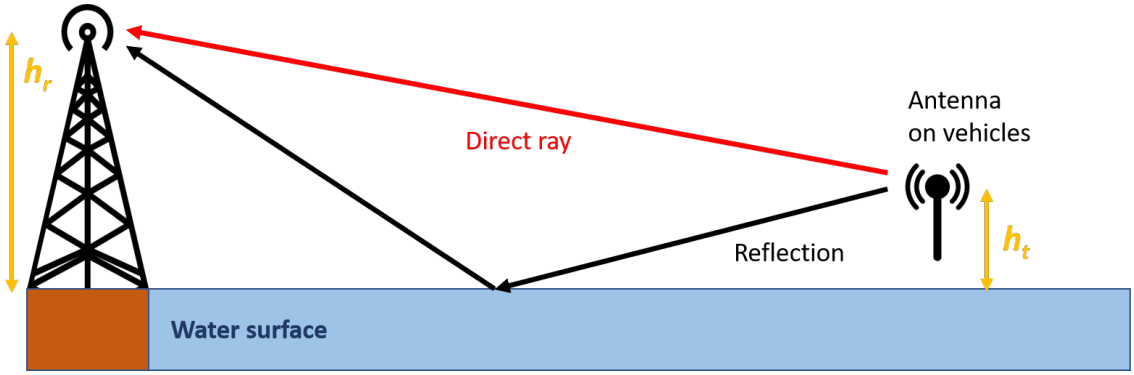

Figure 4.1 *Two-ray representation for near-water surface channel*

loss model. Figure 4.1 describes how this model is characterized. Since a near-grazing incidence appears on the water surface in measurements due to long propagation distances, the reflection coefficient for the radio wave approaches -1. Hence, we can simplify the 2-ray path loss model by formula 4.1:

$$L_{2-ray} = -10log_{10}\left\{\left(\frac{\lambda}{4\pi d}\right)^2\left[2sin\left(\frac{2\pi h_t h_r}{\lambda d}\right)\right]^2\right\}, \tag{4.1}$$

where L_{2-ray} indicates the path loss (dB) calculated by 2-ray model, λ is wavelength in meters and h_t and h_r are the transmitting and receiving antennas heights in meters, respectively.

As the transmitting distance increases beyond d_{break}, 3-ray model becomes a better option. The break point d_{break} indicating the transition point between two models can be estimated using formula 4.2

$$d_{break} = \frac{4h_t h_r}{\lambda}. \tag{4.2}$$

In this 3-ray model, besides the direct path and reflected ray, it also takes into consideration the refracted wave caused by the ducting effects, as shown in Figure 4.2. Among all the duct effects, the evaporation duct is dominant in affecting the near water-surface LOS propagation. Here, this model assumes that the evaporation duct layer is horizontally homogeneous and h_e is effective duct height as shown in Figure 4.2. Then, the 3-ray channel model can simplified as shown in formula 4.3 with the Δ calculated by formula 4.4:

$$L_{3-ray} = -10log_{10}\left\{\left(\frac{\lambda}{4\pi d}\right)^2[2(1+\Delta)]^2\right\}, \tag{4.3}$$

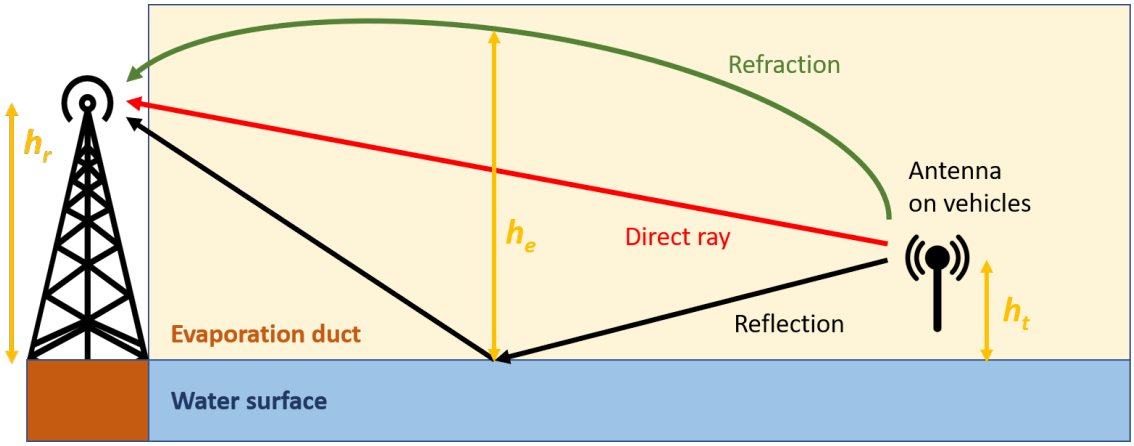

Figure 4.2 *Three-ray representation for near-water surface channel*

with

$$\Delta = 2sin\left(\frac{2\pi h_t h_r}{\lambda d}\right) sin\left(\frac{2\pi(h_e - h_t)(h_e - h_r)}{\lambda d}\right). \tag{4.4}$$

4.1.2 Free space propagation model

In free space propagation model, the transmitter and receiver are assumed to be located in empty environment where no other sources of scattering, diffraction or reflection exists. There should be a clear line of sight between two antennas and no absorbing or reflecting factor should exist [46]. Free space path loss model is one of the commonly used models for ground-to-air radio link [47]. Therefore, in this thesis, this model is used for simulation of the communication from the surface devices to the UAV.

The free space path loss is modeled [46] by applied formula 4.5 as:

$$L_{FSPL} = 32.44 + 20log_{10}(f_c) + 20log_{10}(d), \tag{4.5}$$

where
L_{FSPL}: free space path loss [dB]
f_c: carrier frequency [MHz]
d: distance between transmitter and receiver [km]

4.2 Direct communication between GC and USV

4.2.1 Measurement campaign

The main idea of the first "test" scenario was to observe how well the communication systems operate in near water-surface environment using the beam steering algorithm for new mechanical components on USV side. The RSS and throughput of the USV directional antenna were recorded to evaluate the performance. Besides that, the test was also a preparation for a live demonstration at International Seminar on Safety and Security of Autonomous Vessels (ISSAV) 2019. The idea here is to present the autonomous features of the USV, where the continuous high-speed communication among the devices plays an important role.

The chosen place for the measurement was the Pyhäjärvi lake[2] where the Viikinsaari island[3] is located nearby. The USV part of the communication was installed on the moving vessel and the devices of GC was placed at the harbor[4]. Two laptops were connected to the directional and omni-directional communication interfaces for running scripts to collect RSS and throughput values. Then, we set a predefined route between the harbor and around the island for the vessel to follow. Therefore, we could observe how the system works in both LOS and non-LOS cases.

Figure 4.3 shows the autonomous moving vessel with equipment installed on it. This vessel was provided to the research group by Alamarin-Jet Oy[5]. As can be seen from the image, the directional antenna was installed on the top mast of the boat. In addition, we have also built a dome to cover the USV directional interface. This dome was used to protect the device from weather conditions such as rain, snow or any other kinds of humidity. Besides communication devices, the USV also carried other components on the mast including lidar, surveillance and thermal cameras which were used to enable autonomous capabilities of the water-surface vehicle.

4.2.2 Viikinsaari test results

In the previous section, it was mentioned that the test run at the Pyhäjärvi lake is a preparation step for a live demonstration. At ISSAV 2019 seminar organized at Aalto Univeristy, Finland, we have successfully demonstrated our USV in operation by live streaming on Youtube[6]. Figure 4.4 shows the capture from the live-stream.

[2]Latitude, longitude: 61.483585, 23.726272
[3]Latitude, longitude: 61.4861607,23.6908343
[4]Latitude, longitude: 61.4864526,23.7574103
[5]https://alamarinjet.com/
[6]https://www.youtube.com/watch?v=-CFGQGXHm6k

(a) Final implementation of the USV without the dome on directional antenna

(b) Final implementation of the USV with the dome on directional antenna

Figure 4.3 *Photo of the USV with installed communication equipment*

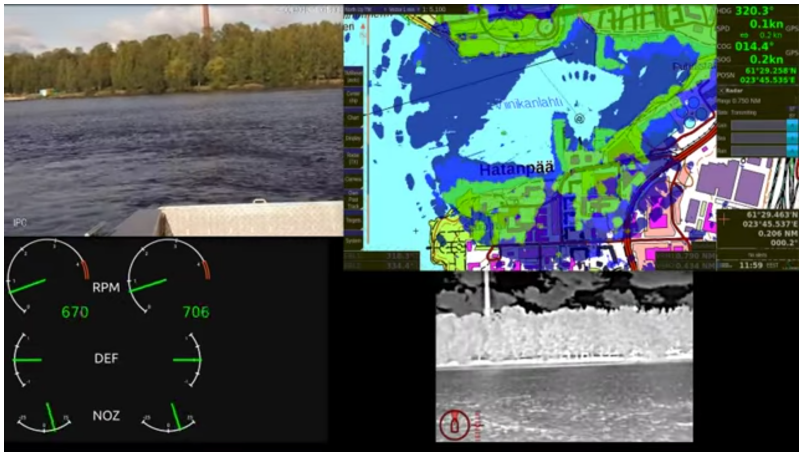

Figure 4.4 *aColor project live-stream screen at ISSAV 2019*

The top left area shows the view of the surveillance camera while the bottom right video is from thermal camera. The record from lidar is in the middle top of the screen. The rest shows the operation parameter of the autonomous water-surface vehicle.

Besides that successful demonstration, the core idea of the test run was to record the Received Signal Strength level and throughput values. Therefore, we had set a route between the ground control and the Viikinsaari island. In this subsection, we discuss the run route and the results in details.

Figure 4.5 illustrates the route which the moving vessel followed during the measurements. The red circle indicated the location of the ground control. The ground control station was equipped with omni-directional antenna installed on a tripod for the simplicity purpose. It was placed on the deck of the nearby harbor. The blue line was the actual route of the USV, which had been plotted by collecting GPS data during the run. The yellow reference points were the intermediate time instants of the measurement, at which the RSS and throughput values will be shown in further plots. The data started to be collected from point 0. The USV moved to the island then circled around it before going back to the GC. The paths from point 0 to point 3 and from point 4 to 7 were Line-of-Sight links for the USV and GC antennas. However, it was non-LOS between point 3 and 4, so those two antennas got disconnected and no GPS data was recorded. Therefore, we illustrate the path between point 3 and 4 as projected path in the Figure 4.5.

Figure 4.6 shows the received signal strength level and throughput results from the test run. The positions on the x-axis indicates the corresponding time instants to the yellow points illustrated in Figure 4.5.

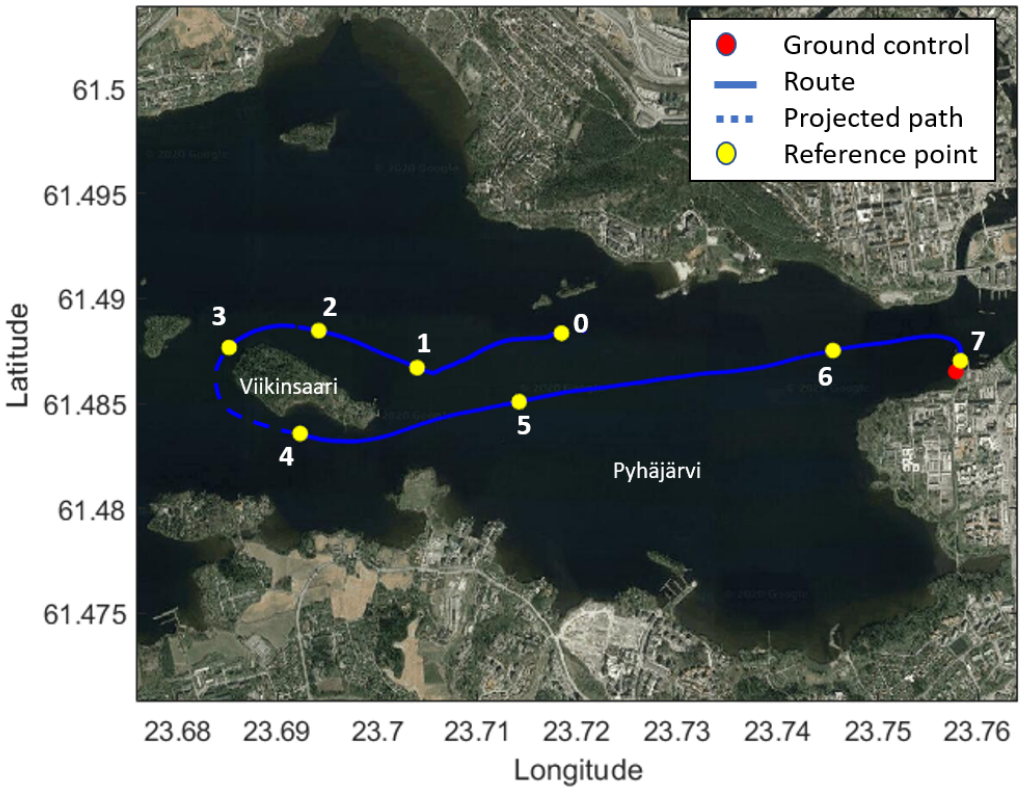

Figure 4.5 *Viikinsaari run route*

Figure 4.6(a) focuses on the RSS level of the directional antenna on the USV. As the water-surface vehicle moves farther away from the GC, the signal level generally decreased (points 0-3). The RSS values fell from -60 dBm to -80 dBm during this period of time. When the boat was moving around the island, the LOS link was blocked. There was no connection between GC and USV, and the RSS dropped immediately below -90 dBm. The connection was re-established after the USV traveled to point 4. The signal level started to gradually increase as the water-surface vehicle was approaching the harbor. We can observe that the values between point 4 and 5 were similar to those of the first part of the measurement as these points were in approximately equal distance to the ground control. In addition, as it can been seen from the graph, there were considerable fluctuations in the plot. This was mainly due to the beam-steering algorithm and the mechanical stability of the antenna affected by the weather conditions and increased speed of the USV.

Figure 4.6(b) shows the throughput results measured by iPerf software[7]. As the recorded throughput values fluctuated drastically, the smooth throughput showed

[7]https://iperf.fr/

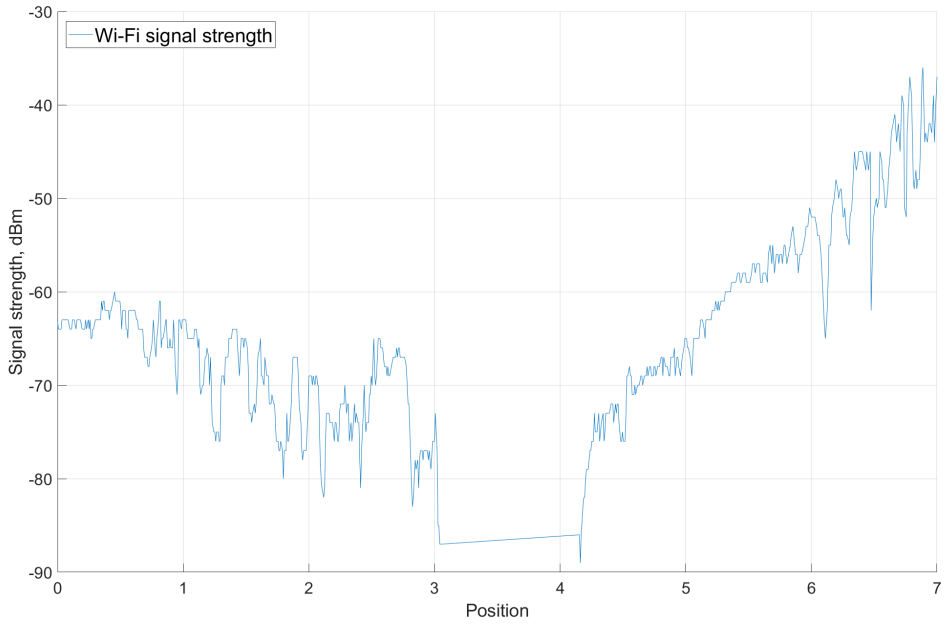

(a) Viikinsaari test run received signal strength level

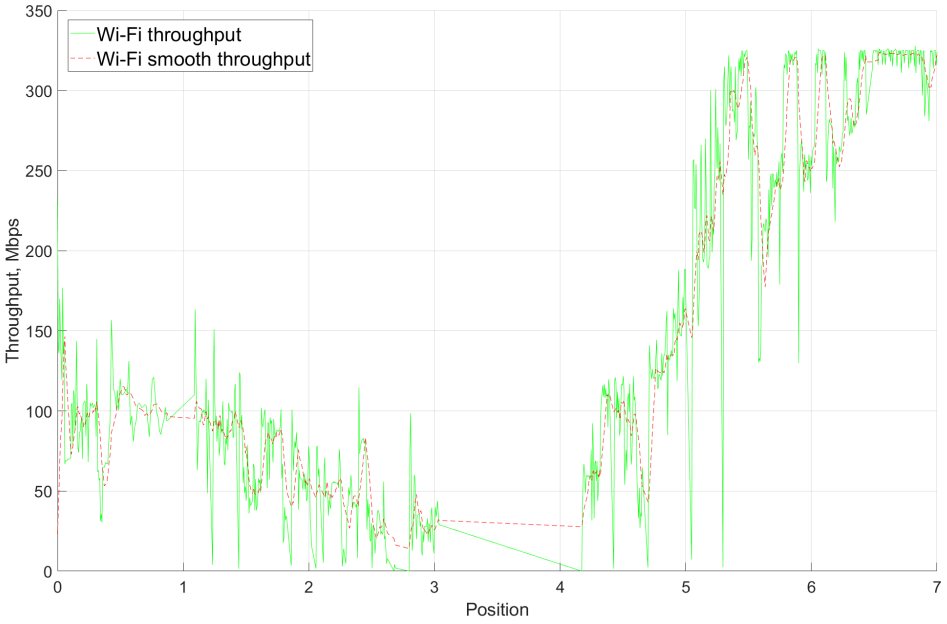

(b) Viikinsaari test run throughput

Figure 4.6 *Measurement results from Viikinsaari test run*

the changing trends of the measurement results. The changing pattern of the plot was similar to the RSS level graph: decreased from point 0 to 3, drop to 0 Mbps between point 3 and 4 and finally increased from point 4 and 7. Generally, the higher signal level connection provided better throughput. When RSS was higher than -60 dBm, the throughput was higher than 150 Mbps. The signal level higher than -50 dBm may make the throughput go up to over 300 Mbps. When the USV lost the LOS link (between position 3 and 4), there were no packets transferred between the ground control and the water-surface vessel leading to the session interruption and zero throughput.

4.2.3 Simulation and evaluation of practical results

The previous section has presented the measurement results of the channel in direct communication between the ground control and the water-surface vehicle. In this section, we compare these results with analytical channel model and discuss the performance results.

As it was mentioned in Section 4.1, we simulated the near water-surface channel model to see its relation to the practical results. In order to get the performance metric of interest (RSS), we needed to first calculate the path loss using Eqs. (4.1)–(4.4). As the practical installment of the devices, the height of transmitter (omni-directional antenna on GC) h_t was 2 m while the height of USV antenna h_r was 3 m. For the duct layer, we decided to follow the values h_e obtained from the study of Lee. et al [45]. After calculating the path loss, the RSS level was determined using formula 2.1. During the Viikinsaari test run, we set the transmission power to be 23 dBm, which makes $P_{tx} + G_{tx}$ = 23 dBm + 12 dBi. This value exceeded the maximum Effective Radiated Power (ERP) set by The Finnish Transport and Communications Agency (TRAFICOM)[8] Regulation 15[9]. However, the MikroTik GrooveA 52 ac had automatically changed the configuration to follow the regulation of current country and region. Therefore, the $P_{tx} + G_{tx}$ sum is 23 dBm. Regarding the gain of the receiver, which is the directional antenna on the USV, its value is 23 dBi assuming that the main beam of the antenna was always pointing to the transmitter. The RSS of near water-surface channel model along with the measured data is illustrated in Figure 4.7.

The blue data line is the result from second part Viikinsaari test run (USV moving from the island to the harbor), which has been plotted against the distance between GC and USV. The drop at 3.5 km indicates the loss of connection between two

[8]https://www.traficom.fi/
[9]https://www.finlex.fi/data/normit/46168/Regulation_15AQ.pdf

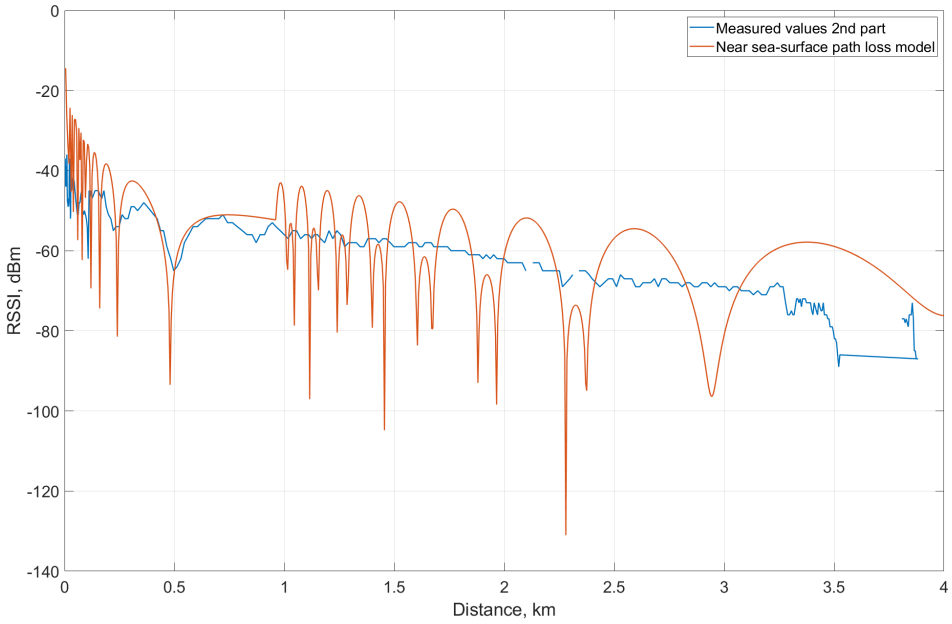

Figure 4.7 *Measured RSS level vs near-water path loss mode*

antennas when the surface vessel was moving behind the island. The RSS level calculated from the theoretical model has two parts separated by the break point at approximately 1 km. We can observe that the simulated signal levels does not match the real ones. The beginning of the red line seems to follow the measurement but after the break point the simulation has completely different pattern. Since the near water-surface channel model is the combination of 2-ray and 3-ray models, we continued to use the 2-ray to compare with the real values. Figure 4.8 shows the RSS of measurement, two-ray model and free space model.

In the graph, change of the RSS from the test run and from the two-ray model follows similar pattern. At some points, values obtained during the measurements were lower than the simulation. This was due to additional noise and interference of the environment. For the distance farther than 3.5 km, the received signal level started to rapidly drop. In addition, the two curves representing measurements and two-ray model are plotted higher than the one obtained from free space model until the distance reaches 3 km. While the reflection ray was positively effecting the RSS, its impact decreases with the distance.

In conclusion, the channel model from the test scenario agrees well with the theoretical two-ray model. Regarding the near sea-surface model, one reason which leads to the mismatch between practical and theoretical results is the difference in the

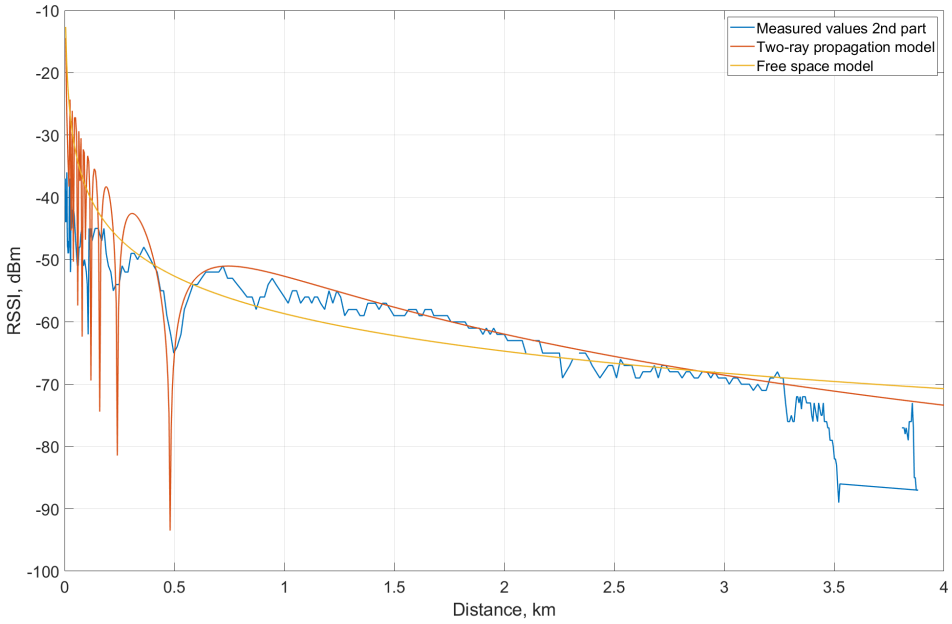

Figure 4.8 *Measured RSS level vs two-ray model and free space model*

height of the transmitter and receiver. In the measurement campaign of Lee. et al [45], the antenna of the ground side is installed at 20 m and 10 m height. Besides that, another factor causing the difference is the distance which the water-surface vehicle travel. The authors of the paper [45] conducted their test run route up to 10 km, which allows them to observe the behavior of the channel in farther range.

4.3 Ground-to-air communication from GC and USV to UAV

4.3.1 Test scenario

After testing the direct communication between the ground control and the unmanned surface vessel, this section focuses on the relay link via unmanned aerial vehicle. The core idea of this test scenario is to observe if the configuration of relay through UAV is able to become a solution in nLOS case.

Since this is a proof of concept, we have conducted the test in the Tampere University, Hervanta campus yard[10]. The Figure 4.9 illustrates the configuration of the system during the measurement. The omni-directional antenna, which was representing USV device, was placed near Tietotalo building while the directional antenna for the ground control was installed near the Konetalo building. Notably, there are

[10]Latitude, longitude: 61.4487267, 23.8578392

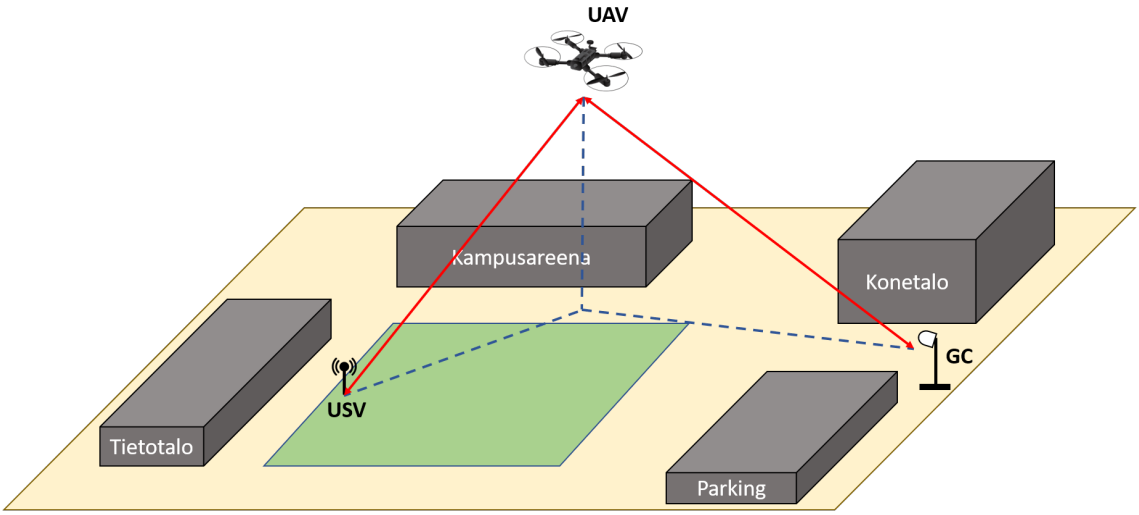

Figure 4.9 *UAV relay test scenario in Tampere University, Hervanta campus*

several obstacles such as automobiles, walls and other structures between assumed GC and USV so these two devices did not have direct LOS to each other. Then, the UAV would fly in front of Kampusareena to relay the communication channel from GC to "USV". The aerial vehicle used in this test is the Quadcopter DJI Matrice 100[11] which was assembled and operated by Unit of Automation Technology and Mechanical Engineering of Tampere University. For the proof-of-concept test, the beam-steering configurations of GC and UAV were pre-calculated and manually set at the devices. The received signal levels of the UAV directional antenna and the omni-directional antenna on the ground were recorded to observe how well the relay system works in the test environment.

4.3.2 Test results

As it was mentioned from previous section, the test run was done to prove the feasibility of the UAV serving as a relay interface between GC and USV in non-LOS case. While the drone was in the air, the two antennas on the ground were successfully connecting and exchanging packets to each other. The Udoo board installed on the UAV was playing an important role of a routing device, which was forwarding packets between the USB Wi-Fi dongle and the Gigabit Ethernet interface connected to MikroTik antenna.

Figure 4.10 shows the recorded RSS levels of the UAV directional antenna and omni-directional antenna on the ground along with the height above takeoff of the drone. There are four positions in Figure 4.10(a) which corresponds to same position in

[11]https://www.dji.com/fi/matrice100

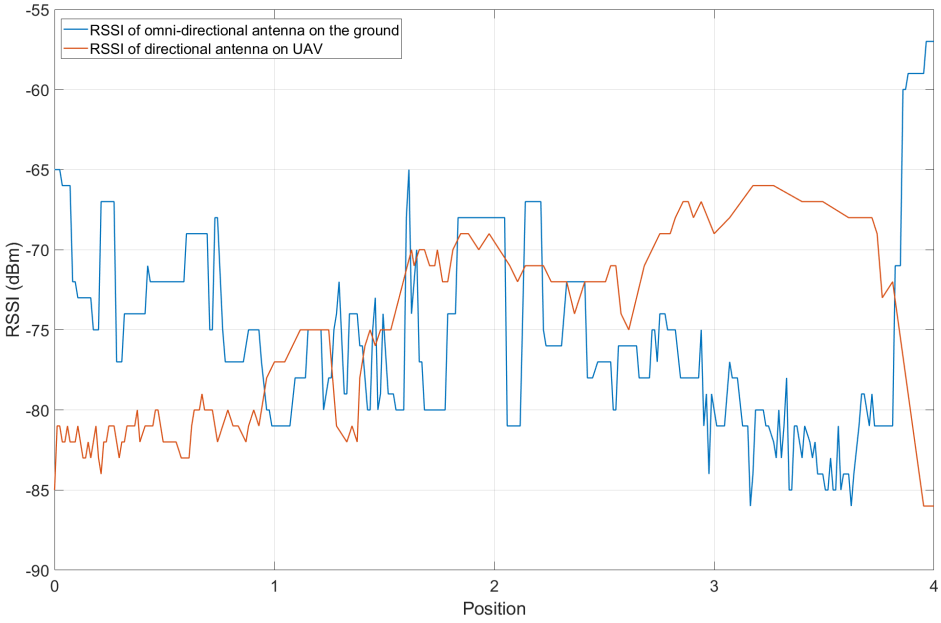

(a) UAV test run received signal strength level

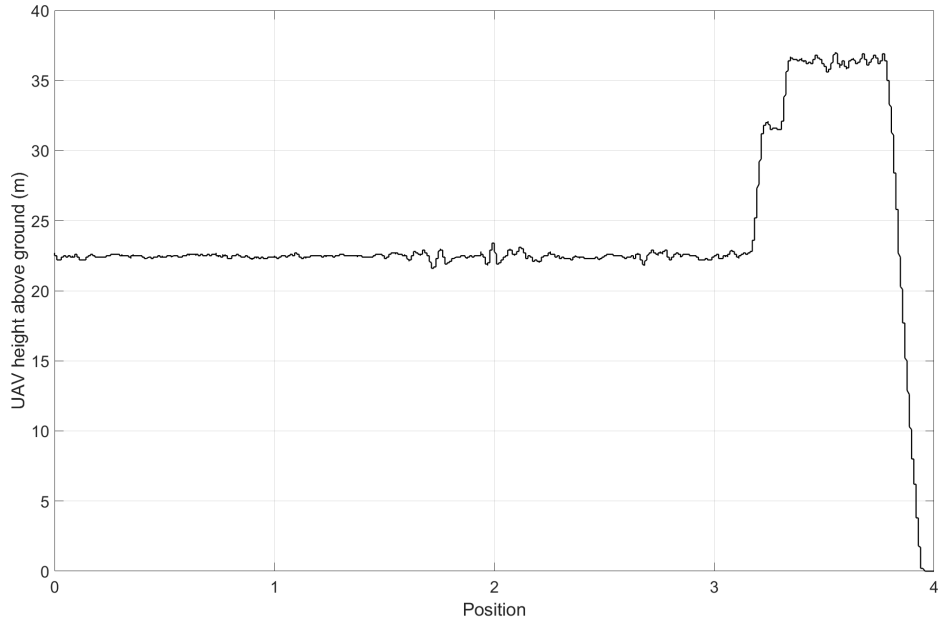

(b) UAV height above takeoff during test run

Figure 4.10 *Measurement results from UAV test in university campus yard*

Figure 4.10(b). In the beginning of the flight (position 1), the aerial vehicle kept the height at 22.5 m above the ground. However, the directional antenna on the drone is not aligned with the directional antenna on GC until position 2. Before that point, the link among 3 devices GC-UAV-USV had already been established even though the GC-UAV RSS considerably low. This is due to the fact that the distance between GC and UAV is short compared to scenario at a wide open space like a lake. The received signal strength of the omni-directional antenna is higher than that of the directional antenna on the drone. Before position 3, we can observe minor changes in the drone altitude. This happened when the flying vehicle was adjusting its yaw. As the beam started to be aligned at point 2, the signal level of the directional antenna was increasing until point 3. When the UAV was increasing its altitude to above 35 m after point 3, the received signal level on the omni-directional interface of the GC decreased while the RSS level at the directional antenna of the UAV was slightly improved. At the end, as the drone was landing, at point 4, the GC and USV antennas lost the line of sight so the signal level dropped immediately. Meanwhile, the RSS of omni-directional antenna increased significantly.

The changes in signal strength of the omni-directional antennas against the drone altitude appear due to radiation pattern. Omni-directional antennas used in this study are effectively a dipole-like antennas and have a toroid-like radiation pattern, being omni-directional only in horizontal plane. Therefore, the received signal becomes weaker, when the devices are more separated in a vertical plane. That is the reason why the RSS in the test drops when the aerial vehicle increases its height above the ground and instantly rises as the UAV lands.

The connection between GC and USV depends on two ground-to-air radio links: between GC and UAV and between USV and UAV. The results from the test show that one of them (with lower RSS) will always be a bottleneck link, which limits the throughput of the overall relay system. Therefore, the position of the UAV should be figured out to optimize the bottleneck radio link.

4.3.3 UAV positioning analysis

As it is mentioned in previous section, in the relay situation, there exists a bottleneck radio link. Since in practical deployment the UAV will be autonomous and programmed to follow the USV, we need to find out the optimal position of the aerial vehicle in relation to the moving vessel and GC so that the quality of the connection can be maintained. In this section, we discuss and evaluate the simulation reflecting the RSS of the relaying scenario with varying UAV position, that can maximize the bottleneck received signal level.

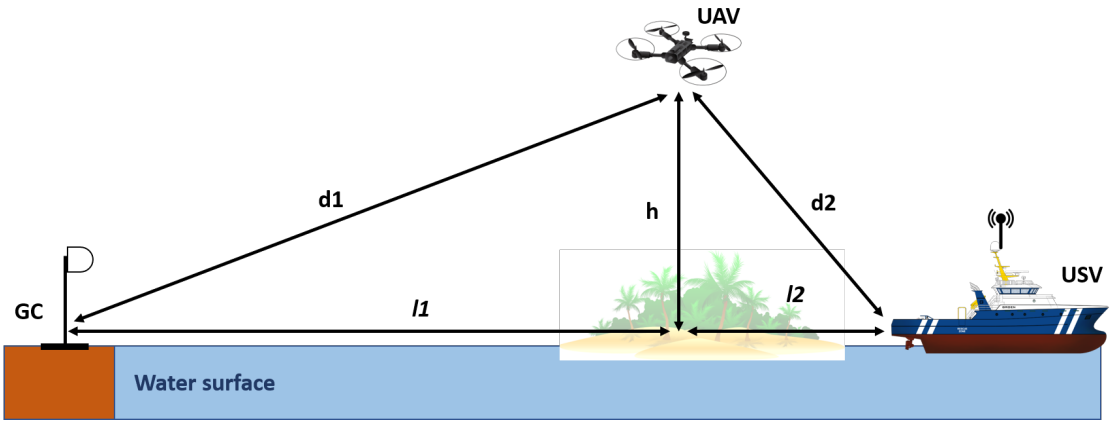

Figure 4.11 *Simulation scenario for finding optimized UAV position to the USV*

Figure 4.11 illustrates the position assumption for the vehicles in the simulation. The channel model used to simulate GC-UAV and UAV-USV connections is free space model since the ground-to-air radio links in this situation are in line of sight and open space environment. The distance between the ground control, the obstacle (the island) and the water-surface vehicle follow the Viikinsaari test run, so the $l1$ and $l2$ are set 3 km and 1 km, respectively. The UAV is assumed to fly at altitude $h = 22.5$ m above the ground, which is higher than the average tree and other infrastructure level on the island, to maintain the LOS with both GC and USV. The two values $d1$ and $d2$ are calculated based on the parameters above. In the simulation, the two values $l1$ and $l2$ vary from 0 to 4 km, which indicates the installed location of GC and movement of USV. The RSS levels of the GC-UAV and UAV-USV links are calculated based on free space model and then compared to each other. The one with lower signal level is the bottle neck which will be plotted on a graph against $d1$ and $d2$.

Figure 4.12 shows the bottleneck RSSI of the communication system. Generally, it is visible from the graph that the RSSI increases as the $d1$ and $d2$ distance decreases. Area A in the figure implies the cases when the bottleneck received signal strength only depends on $d1$ regardless the $d2$ value. In area B, the received signal strength values are subject to the UAV-USV distance. For each constant $d1$, as the distance $d2$ between the drone and the boat increases (crosses the red line), the UAV-USV link becomes the bottleneck for the overall system and the RSS values become lower than those in area A. Hence, we need to keep $d2$ distance to be on the left of the red line. That line represents the optimal RSSI while the GC-UAV-USV distances are growing. To find the relation of $d1$ and $d2$ on that line, each ($d1$,$d2$) pair on the red line is collected and parsed to a curve fitting function in Matlab. The function *polyfit()* in Matlab is used for this purpose to calculate the coefficients

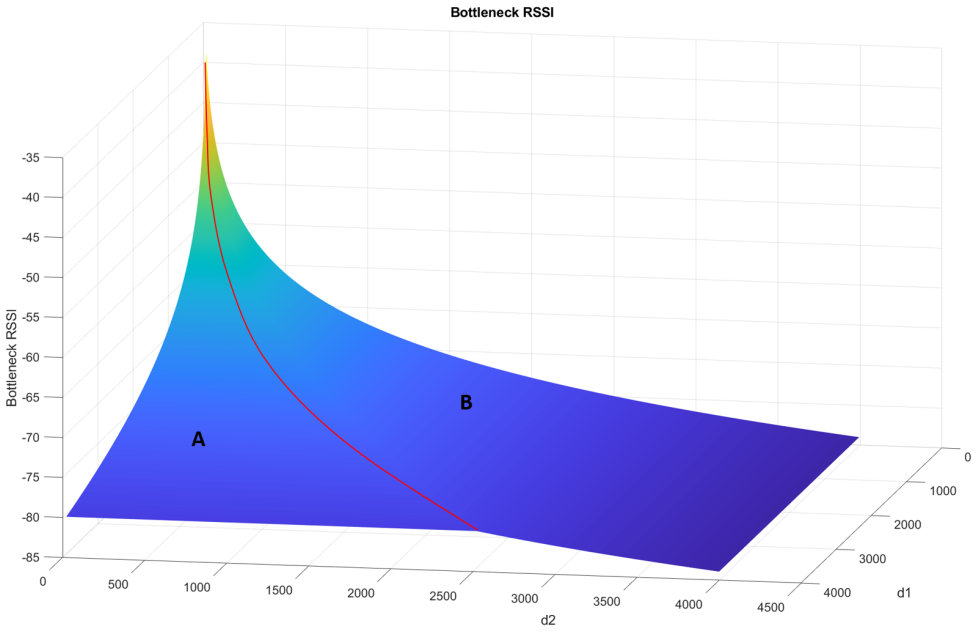

Figure 4.12 *Bottleneck RSSI of the overall radio link*

of a polynomial that best fit the input data. Then, the line can be estimated as $d_2 = 0.6309d_1 - 0.1954$, with $d1$ and $d2$ measured in kilometers. Thus, with current antenna setup and transmitter power settings, the UAV should keep its distance to the USV to be equal to or shorter than $0.6309d_1 - 0.1954$ to optimize the overall RSSI of the system. The relation for optimal $d1$ and $d2$ can be expressed as:

$$d_2 \leqslant 0.6309d_1 - 0.1954, \tag{4.6}$$

Using the estimated optimal position of the drone against the water-surface vessel, we simulated the bottleneck RSSI of the relay link and compared it with the measured RSSI. The x-axis features the horizontal distance l between the ground control and the water vessel, which means $l = l1 + l2$. Using that along with the height and the relation $d_2 = 0.6309d_1 - 0.1954$ from above, we can find a pair of $(l1, l2)$ and ($d1$,$d2$) for each distance l. From those values, the path loss values for GC-UAV and UAV-USV are calculated and the lower ones were collected as a basis for RSSI to be plotted. Figure 4.13 presents the mentioned comparison. From the graph, we can see that as the moving vessel loses the line of sight with distance farther than 3.5 km, the relay link (red curve) works better than the direct link (blue curve) and becomes a solution to maintain the connection between the ground control and the water vehicle. However, the direct link performs better than the relay link at distances below 3.5 km. The reason for this is the lower reception gain of

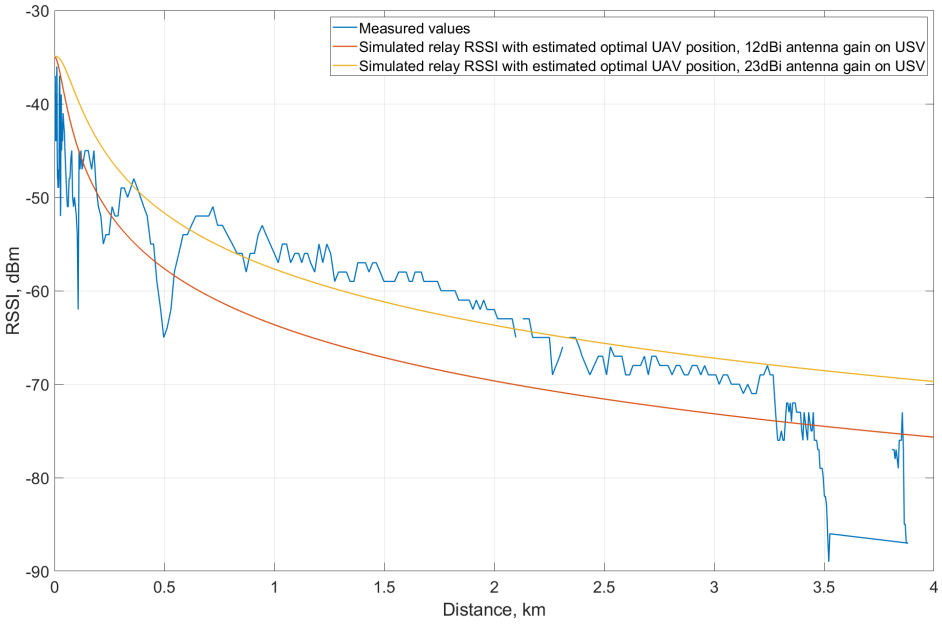

Figure 4.13 *Comparison of measured RSS and simulated relay RSS*

the USV and UAV antenna used in relay case. In the scenario with direct GC-USV connection, the antenna on USV is directional and the gain of the main lobe is 23 dBi while in relay system, the reception gain is 16 dBi for the directional antenna on the UAV and 12 dBi for the omni-directional antenna on USV. The use of 12 dBi omni-directional antenna on USV also limits the possible UAV-USV distance, which creates imbalance between optimal distance values for the relay connection components. While the unmanned flying vehicle has to keep its proximity to the autonomous boat, the range between the GC and the UAV becomes significantly farther than UAV-USV distance. The 16 dBi directional antenna on the UAV cannot compensate that distance to provide an adequate signal strength compared to the 23 dBi one in the direct case, which leads to the comparison of direct and relay cases to be unfair in terms of equipment settings.

Therefore, we made another comparison between direct and relay scenarios with equal conditions of GC and USV. Assuming that the effective radiated power from the transmitter (ground control) are the same for both cases, the USV now will be assumed to use 23 dBi directional antenna on a UAV-USV link. Using the same approach mentioned previously, the simulated relay RSSI is illustrated with yellow curve in Figure 4.13. From the graph, we can observe that the relay system with 23 dBi directional antenna on USV performs better than the direct link when the boat is 2 km farther than the ground control. In this case, with higher receiving

gain in USV, the range of UAV against the water-surface vehicle is extended and the GC-UAV and UAV-USV links in relay scenario are now more balanced in terms of optimal range.

Knowing the optimal position of the UAV in reference with the boat provides ideas on how the UAV should be used in autonomous collaborative offshore network. To prevent the signal loss, or session interruption in nLOS case, the boat should predict that there will be obstacles blocking the channel based on the map calculations and then deploy the drone in advance to maintain the connection between the ground control and the water vehicle. After being launched, the UAV follows the boat within a range which is calculated based on the distance between the water vessel and the ground control using the optimal position found above. Another usage of the drone is to extend the coverage of the wireless system. As it was indicated previously, with higher USV antenna gain, the relay system can perform better than direct link in farther distances. Therefore, the boat can deploy the drone to improve the connection quality when the RSS is dropping below a defined value.

5 Conclusions

This chapter presents the conclusion summarizing the thesis. This research work is a part of the aCOLOR project which aims to prototype a novel intelligent ecosystem for water environment. To support the offshore monitoring and unmanned operations, the designed system focuses on the high speed and long range aspect of Machine-Type Communications.

To achieve the goals mentioned above, this master thesis has summarized the process of design, implementation and evaluation of a wireless communication system for autonomous maritime robotics. The core components of the system analyzed in the scope of the thesis are Unmanned Surface Vessel and Unmanned Aerial Vehicle along with the Ground Control. There are two communication modes: direct mode and relay mode. The first one implies that there is a direct LOS link between GC and USV. The relay mode is established when there is no direct connection (nLOS); in that case, the UAV is deployed to act as a relay node. The radio interfaces used in the project are based on the IEEE 802.11 Wi-Fi standard working in 5 GHz frequency bands. To establish and maintain the desired communication link, directional antennas were used to enable the high throughput connection over a long distance. For that purpose, each unmanned vehicle in the offshore system is equipped with the appropriate communication unit. Generally, this module incorporates wireless interfaces for communication, rotation mechanism for mechanical beam-steering and a controller for data collection and processing. The similar modules are placed on GC, USV and UAV. The specific design of each communication unit depends on the vehicle on which it is installed. The detailed explanation of the implementation of the system mentioned above is described in Section 3.

After the system was implemented, we conducted practical tests for LOS and NLOS scenarios. Based on the measurement campaign done for LOS case scenario, we can conclude that the system performed satisfactorily. The throughput varies from 100 Mbps to 300 Mbps. That connection speed is adequate for transmitting sensors data and streaming live HD-quality videos. Moreover, the results show that the direct radio link between the GC and USV matches with theoretical two-ray channel model. For the second case, we performed a proof-of-concept relay test at the university campus and demonstrated that the designed relay system works. Moreover, based on the test results, we concluded that there always be a bottleneck link, limiting the performance of the relay system. Therefore, we have used the simulation to find out the optimal UAV position between the USV and GC to improve the bottleneck con-

nection. Section 4 presents detailed discussion on the measurement and simulation results for two mentioned tests.

To complete the communication system implementation, the next logical step in the project is to conduct a test in maritime environment to observe how the relay system performs in nLOS scenario. Besides that, as the autonomous vessel will experience both LOS and nLOS while travelling, it is necessary to develop a handover mechanism between direct and relay modes to maintain the continuous connection between the devices. The simple and reliable logic could be based on the RSS measurements. As an example, the simple threshold-based mechanism could be employed: if the RSS goes below a pre-defined threshold, the system will switch from direct mode to relay mode. Moreover, as a part of the aCOLOR project, the next stage is also to implement the communication system on the Autonomous Underwater Vehicle; thus, to include the final component enabling the inter-connectivity for fully autonomous offshore ecosystem.

References

[1] *IMT traffic estimates for the years 2020 to 2030*. ITU-R M.2370. 2015.

[2] Bernhard Raaf et al. "Vision for Beyond 4G broadband radio systems". In: *IEEE International Symposium on Personal, Indoor and Mobile Radio Communications, PIMRC*. 2011. ISBN: 9781457713484. DOI: 10.1109/PIMRC.2011.6139944.

[3] Zaher Dawy et al. "Toward Massive Machine Type Cellular Communications". In: *IEEE Wireless Communications* (2017). ISSN: 15361284. DOI: 10.1109/MWC.2016.1500284WC.

[4] O. N. C. Yilmaz et al. "Analysis of ultra-reliable and low-latency 5G communication for a factory automation use case". In: *2015 IEEE International Conference on Communication Workshop (ICCW)*. 2015, pp. 1190–1195. DOI: 10.1109/ICCW.2015.7247339.

[5] Alberto Reche et al. "A Smart M2M Deployment to Control the Agriculture Irrigation". In: *Ad-hoc Networks and Wireless*. Ed. by Miguel Garcia Pineda et al. Berlin, Heidelberg: Springer Berlin Heidelberg, 2015, pp. 139–151. ISBN: 978-3-662-46338-3.

[6] A. Ahad, M. Tahir, and K. A. Yau. "5G-Based Smart Healthcare Network: Architecture, Taxonomy, Challenges and Future Research Directions". In: *IEEE Access* 7 (2019), pp. 100747–100762. DOI: 10.1109/ACCESS.2019.2930628.

[7] Antonio Vasilijević et al. "Coordinated navigation of surface and underwater marine robotic vehicles for ocean sampling and environmental monitoring". In: *IEEE/ASME Transactions on Mechatronics* (2017). ISSN: 10834435. DOI: 10.1109/TMECH.2017.2684423.

[8] Helen Hastie et al. "The ORCA Hub: Explainable Offshore Robotics through Intelligent Interfaces". In: (Mar. 2018).

[9] GMDT Forecast. "Cisco visual networking index: global mobile data traffic forecast update, 2017–2022". In: *Update* 2017 (2019), p. 2022.

[10] Tarik Taleb and Andreas Kunz. "Machine type communications in 3GPP networks: Potential, challenges, and solutions". In: *IEEE Communications Magazine* (2012). ISSN: 01636804. DOI: 10.1109/MCOM.2012.6163599.

[11] P. Jain, P. Hedman, and H. Zisimopoulos. "Machine type communications in 3GPP systems". In: *IEEE Communications Magazine* 50.11 (2012), pp. 28–35. DOI: 10.1109/MCOM.2012.6353679.

[12] Ivan Jovovic, Ivan Forenbacher, and Marko Periša. “Massive Machine-Type Communications: An Overview and Perspectives Towards 5G”. In: Oct. 2015. DOI: 10.18638/rcitd.2015.3.1.73.

[13] H. Shariatmadari et al. “Machine-type communications: current status and future perspectives toward 5G systems”. In: *IEEE Communications Magazine* 53.9 (2015), pp. 10–17. DOI: 10.1109/MCOM.2015.7263367.

[14] Matthew S. Gast. *802.11 Wireless Networks: The Definitive Guide, 2nd Edition*. eng. 2nd ed. O’Reilly Media, Inc, 2005. ISBN: 9780596100520.

[15] By Matthew Gast. *Wireless Networks: The Definitive Guide*. 2002. ISBN: 0-596-00183-5.

[16] Jon Rigelsford. “802.11 Wireless Networks: The Definitive Guide”. In: *Sensor Review* (2003). ISSN: 0260-2288. DOI: 10.1108/sr.2003.08723bae.003.

[17] Y. Ghasempour et al. “IEEE 802.11ay: Next-Generation 60 GHz Communication for 100 Gb/s Wi-Fi”. In: *IEEE Communications Magazine* 55.12 (Dec. 2017), pp. 186–192. ISSN: 1558-1896. DOI: 10.1109/MCOM.2017.1700393.

[18] Joachim Sachs et al. “5G Radio Network Design for Ultra-Reliable Low-Latency Communication”. eng. In: *IEEE network* 32.2 (2018), pp. 24–31. ISSN: 0890-8044.

[19] Ekaterina Markova et al. “Analyzing impact of path loss models on probability characteristics of wireless network with licensed shared access framework”. In: *International Congress on Ultra Modern Telecommunications and Control Systems and Workshops*. 2017. ISBN: 9781538634349. DOI: 10.1109/ICUMT.2017.8255189.

[20] *Wireless Communications: Principles and Practice*. Prentice Hall communications engineering and emerging technologies series. Dorling Kindersley, 2009. ISBN: 9788131728826. URL: https://books.google.fi/books?id=11qEWkNFFwQC.

[21] A. L. Grant. “Path Loss Models for Two Small Airport Indoor Environments at 31 GHz”. MA thesis. University of South Carolina, 2019.

[22] Lars Ahlin, Jens Zander, and Slimane Ben Slimane. *Principles of Wireless Communications*. QC 20111130. Studentlitteratur, 2006, p. 734. ISBN: 91-44-03080-0.

[23] Martin Grabner and Vaclav Kvicera. “Atmospheric Refraction and Propagation in Lower Troposphere”. In: June 2011. ISBN: 978-953-307-304-0. DOI: 10.5772/16379.

[24] Yee Hui LEE and Yu Song MENG. “Empirical Modeling of Ducting Effects on a Mobile Microwave Link Over a Sea Surface”. eng. In: *Radioengineering* 21.4 (2012), pp. 1054–1059. ISSN: 1210-2512.

[25] Yu Song Meng and Yee Hui Lee. “Measurements and Characterizations of Air-to-Ground Channel Over Sea Surface at C-Band With Low Airborne Altitudes”. eng. In: *IEEE Transactions on Vehicular Technology* 60.4 (2011), pp. 1943–1948. ISSN: 0018-9545.

[26] H.V Hitney and L.R Hitney. “Frequency diversity effects of evaporation duct propagation”. eng. In: *IEEE Transactions on Antennas and Propagation* 38.10 (1990), pp. 1694–1700. ISSN: 0018-926X.

[27] Saleh Faruque and Saleh Faruque. *Radio Frequency Modulation Made Easy*. 2016. ISBN: 9783319412009.

[28] Simon R. Saunders. *Antennas and propagation for wireless communication systems*. eng. 2nd ed. Chichester: Wiley. ISBN: 0470848790.

[29] Andrew Butterfield, Gerard Ekembe Ngondi, and Anne Kerr. *A Dictionary of Computer Science (7 ed.)* Oxford University Press, 2016. DOI: 10.1093/acref/9780199688975.001.0001.

[30] Patrick Killelea. *Web Performance Tuning, 2nd Edition*. O’Reilly Media, Inc., 2002. ISBN: 9780596001728.

[31] Guowang Miao et al. *Fundamentals of mobile data networks*. 2016. ISBN: 9781316534298. DOI: 10.1017/CBO9781316534298.

[32] *An Introduction to Computer Networks*. Open textbook available at: http://intronetworks.cs.luc.edu/. 2020.

[33] Larry L. Peterson and Bruce S. Davie. *Computer Networks, Fifth Edition: A Systems Approach*. 5th. San Francisco, CA, USA: Morgan Kaufmann Publishers Inc., 2011. ISBN: 0123850592.

[34] Peter Singerl and Christian Vogel. “An Analysis of a Low Complexity Received Signal Strength Indicator for Wireless Applications”. In: Oct. 2004.

[35] Zhanyong Tang et al. “Exploiting Wireless Received Signal Strength Indicators to Detect Evil-Twin Attacks in Smart Homes”. In: *Mobile Information Systems* (2017). ISSN: 1875905X. DOI: 10.1155/2017/1248578.

[36] Petar Popovski et al. “Wireless Access for Ultra-Reliable Low-Latency Communication: Principles and Building Blocks”. eng. In: *IEEE network* 32.2 (2018), pp. 16–23. ISSN: 0890-8044.

[37] Behrouz A Forouzan. *Data Communications and Networking*. eng. Place of publication not identified: McGraw Hill Science Engineering & Mathematics Imprint. ISBN: 0-07-149018-3.

[38] James F. Kurose. *Computer networking : a top-down approach*. eng. 5th, international ed. New York: Pearson. ISBN: 978-0-13-136548-3.

[39] *TechFinland100, 2018. Autonomous and Collaborative Offshore Robotics (aCOLOR)*. Available at: https://techfinland100.fi/acolor-autonomous-air-water-surface-and-underwater-inspections/. TechFinland100. 2019.

[40] Jose Villa Escusol et al. "aColor: Mechatronics, Machine Learning, and Communications in an Unmanned Surface Vehicle". In: Mar. 2020.

[41] Jose Villa Escusol, Jussi Aaltonen, and Kari Koskinen. "Model-based path planning and obstacle avoidance architecture for a twin jet Unmanned Surface Vessel". In: Mar. 2019. DOI: 10.1109/IRC.2019.00083.

[42] Zeinab Khosravi et al. "Designing high-speed directional communication capabilities for unmanned surface vehicles". In: *Proceedings of the International Symposium on Wireless Communication Systems*. 2019. ISBN: 9781728125275. DOI: 10.1109/ISWCS.2019.8877304.

[43] *Movable Type Scripts: Calculate distance, bearing and more between Latitude/-Longitude points*. Available at: http://www.movable-type.co.uk/scripts/latlong.html/.

[44] *How To Calculate Distances, Azimuths and Elevation Angles Of Peaks*. Available at: tchester.org/sgm/analysis/peaks/how_to_get_view_params.html.

[45] Yee Hui Lee, Feng Dong, and Yu Song Meng. "Near sea-surface mobile radiowave propagation at 5 GHz: Measurements and modeling". In: *Radioengineering* (2014). ISSN: 12102512.

[46] J. D. Parsons. *The Mobile Radio Propagation Channel*. 2001. DOI: 10.1002/0470841524.

[47] Zhuangzhuang Cui et al. "Low-altitude UAV air-ground propagation channel measurement and analysis in a suburban environment at 3.9 GHz". In: *IET Microwaves, Antennas and Propagation* (2019). ISSN: 17518733. DOI: 10.1049/iet-map.2019.0067.

APPENDIX A. Calculation of the tilting angle of the directional antenna on USV

Program 1 *Calculation of the tilting of the directional antenna on USV*

```
# Import packages and libraries
import numpy as np
from math import cos, atan2, pi, sin, atan
from modules import LSM9DS0

def calculate_tilt_angle(rotation_angle):
    orientation=get_orientation()
    pitch = orientation[1]
    roll = orientation[0]
    rotation = np.radians(rotation_angle)

    # Vectors u and v define our plane according to
    # the pitch and roll of the boat
    u = np.array([0, np.cos(pitch), np.sin(pitch)])
    v = np.array([np.cos(roll), 0, np.sin(roll)])

    # Vector d is pointing to the direction
    # the antenna is turned on the xy-plane
    d = np.array([np.cos(rotation), np.sin(rotation), 0])

    # Vector n is orthogonal to our plane
    n = np.cross(u, v) / np.linalg.norm(np.cross(u, v))

    # Projection tells us where the antenna
    # is pointing in the xyz-space
    projection = [d[0], d[1], np.dot(n/-n[2], d)]

    # This tells us how much
    # the antenna is tilted up or down
    angle = np.degrees(np.arccos(np.dot(d, projection)/
    np.linalg.norm(d) / np.linalg.norm(projection))) *
    np.sign(projection[2])
    return angle
```